Engineering Fracture Mechanics 79 (2012) 389–414

Contents lists available at SciVerse ScienceDirect

Engineering Fracture Mechanics

journal homepage: www.elsevier.com/locate/engfracmech

Non linear fracture mechanics of polymers: Load Separation and Normalization methods

Patricia María Frontini *, Laura Alejandra Fasce, Federico Rueda

Instituto Nacional de Investigaciones en Ciencia y Tecnología de Materiales INTEMA, Universidad Nacional de Mar del Plata, CONICET, Av. J.B. Justo 4302, B7608FDQ Mar del Plata, Argentina

ARTICLE INFO

Article history:
Received 23 June 2011
Received in revised form 16 November 2011
Accepted 23 November 2011

Keywords:
Ductile polymers fracture toughness testing
J-Integral approach
R curves
Normalization method
Load Separation method

ABSTRACT

Fracture toughness of ductile polymers can be measured by the incremental crack growth resistance curve, where *J-Integral* value is plotted as a function of crack extension. The determination of the resistance curve, *J–R*, is generally performed through the so-called multiple-specimen technique. In this procedure, several identical specimens are loaded to obtain different amounts of crack growth, thus involving a large number of tests and large quantity of test material. It is also hard to apply in situations such as under high-loading rate conditions, elevated temperatures and/or aggressive environments where it is difficult to stop the test to measure crack extension. Consequently, alternative single specimen techniques appear attractive. The theoretical basis for the single specimen *J* form used in the incremental *J–R* curves is given by the Load Separation Principle. It is based on the assumption that the load can be represented as the multiplication of two separate functions: a crack geometry function and a material deformation function. This principle allows the introduction of the so-called η parameter which greatly simplifies *J* calculation. The crack geometry function is general represented as a power law function which exponent coincides with η factor. By analyzing load line displacement records of several blunt notched specimens differing in their initial crack length before the starting of crack propagation it is possible to evaluate η factor and verify Load Separation Principle assumption. Based on the validity of this principle two methodologies have been developed: Load Separation method, S_{pb}, and Normalization Data Reduction technique. These methodologies have the inherent advantage of developing *J–R* curves directly from a single load versus load-line displacement record without using any sophisticated automated crack length monitoring system. Load Separation method infers the growing crack length from the load ratio of two load–displacement records: one growing crack and other stationary crack. Normalization method utilizes the Material Key Curve, calibrated using one individual normalized load–displacement record, to infer the instantaneous crack length. Variants of both methodologies have been already successfully used in ductile fracture characterization of polymers by several authors.

Abbreviations: A110, annealed at 110 °C; A150, annealed at 150 °C; A90, annealed at 90 °C; ABS, acrylonitrile butadyene styrene terpolymer; Al, aluminum; AS, Arc-shaped specimens; ASTM, American Society for Testing and Materials; CM, compression molded; CT, compact tension specimen; EM, extrusion molded; EPBC, ethylene–propylene block copolymer; ESIS TC4, European Structural Integrity Society Technical Committee for Polymers and Polymer Composites; HDPE, high density polyethylene; HIPS, high impact polystyrene; IM, injection molded; LEFM, linear elastic fracture mechanics; MIPS, medium impact polystyrene; NPr, non-proportional specimens; PC, polycarbonate; PCTFE, poly(chlorotrifluoroethylene); PEEK, poly(etheretherketone); PPBC, polypropylene block copolymer; PPc, propylene copolymer; PPH, polypropylene homopolymer; Pr, proportional specimens; PTFE, (poly)tetrafluoroethylene; PVC, poly(vinylchloride); PVDF, poly(vinylidenefluoride); RTAN, rubber-toughened amorphous nylon; RTN66, rubber-toughened nylon 6/6; R-curve, material resistance curve; RT-Nylon, rubber-toughened nylon; RT-PMMA, rubber-toughened poly(methylmetacrylate); *SBZ*, stable blunting zone; SG, side grooved specimens; S_{pb}, Load Separation method; SE(B), single edge bending specimen test configuration; UHMWPE, ultrahigh molecular weight polyethylene.

* Corresponding author. Fax: +54 223 4810046.
E-mail addresses: pmfronti@fi.mdp.edu.ar (P.M. Frontini), lfasce@fi.mdp.edu.ar (L.A. Fasce), federico.rueda@fi.mdp.edu.ar (F. Rueda).

0013-7944/$ - see front matter
doi:10.1016/j.engfracmech.2011.11.020

Innovatively here, the Load Separation Principle and the deformation function are expressed in terms of total displacement without distinguishing between elastic and plastic displacement components. Hence, calculations are simply made using the *J-Integral* formula based on total energy. The performance of the proposed methods is evaluated and compared with the standard multiple-specimen technique for a broad spectrum of ductile polymers. Several features of the approaches are discussed like: suitability of functional forms, influence of blunting assumption, calibration points and general limitations to their application. The results demonstrate the ease and the accurate of the Normalization method based on total displacement for ductile polymer *J–R* curve determination. Conversely, the great potentiality of Load Separation method relies on the special fracture cases in which the actual final crack length cannot be easily determined.

1. Introduction

To use polymers in load bearing industrial applications with confidence, reliable mechanical characterization is necessary. Manufactured structures irremediably contain flaws that govern eventual structural failure. The ability of a material to resist such a failure can be interpreted in terms of fracture toughness. Fracture toughness is a measurement of the energy required to deform a material, and that deformation ultimately leads to crack propagation. Higher fracture toughness equals higher resistance to crack growth, which can be equated to higher performance. Much work has been done during the past decades in an effort to find fracture characterization properties for engineering materials. Fracture mechanics provides mathematical relationships between stress, flaw size and toughness which are used to predict the behavior of a structural component from the results of laboratory tests.

Tough thermoplastics – rubber modified glassy polymers and semi crystalline polymers – exhibit non linear behavior due to strong viscoelastic-viscoplastic behavior and /or significant crack tip plastic deformation during crack propagation. Besides, they allow the crack to propagate with large extension. Thus, fracture toughness determination implies the application of non-linear theories. Among others [1–4], one suitable approach is the so-called *J-Integral* fracture toughness criterion [5–9]. Besides being the most widely used approach to define fracture toughness of non-linear materials, *J-Integral* is also suitable in structural integrity assessment under non-linear conditions [10,11].

The *J-Integral* method was originally proposed by Rice [8,9] as a means of characterizing the stress–strain singularity at a crack tip in a non linear elastic material. It expresses the energy per unit area necessary to create new fracture surfaces in a loaded body containing a crack. At crack initiation, it may be determined from considering the load–deflection curves of two bodies with crack lengths of a and $a + da$, as follows:

$$J = -\frac{1}{b}\frac{\partial U}{\partial a}\bigg|_{v} \tag{1}$$

where v is the displacement, U is the potential energy of the loaded body (the energy given by the area under the load–deflection curve), b is the un-cracked ligament length, and $J = J_c$ at fracture. *J-Integral* was proposed as a fracture criterion for the elastic–plastic behavior of metals and extended the linear elastic fracture mechanics (LEFM) concepts to cases in which large scale plasticity is involved. It constitutes a material parameter corresponding to the energy required to produce a unit area of new crack surface.

Based on Eq. (1) Begley and Landes developed the so-called multiple-specimen method [12,13] to measure fracture toughness. Due to its inherent difficulty, this method was rapidly replaced by the simpler single-specimen technique developed by Rice et al. [14] and Merkle and Corten [15]. Using limit load analysis they were able to develop a new form for J:

$$J = \frac{\eta}{b}\int M\,d\theta \tag{2}$$

where θ is the additional rotation due to the presence of the crack and M is the bending moment, b is the un-cracked ligament length, η is a function of crack length to width ratio. Finally, Sumpter and Turner proposed the following expression for J [16]:

$$J = \eta_{el}\frac{A_{el}}{b} + \eta_{pl}\frac{A_{pl}}{b} \tag{3}$$

where A_{el} and A_{pl} are the elastic and plastic parts of the area under the load-line displacement record, respectively, and η_{el} and η_{pl} are functions of crack length to width ratio, a/W. This alternative procedure for the experimental estimation of J significantly simplified J calculation.

In highly ductile materials where crack grows stably the process of defining an initiation condition involved to develop the crack growth resistance curve (R-curve), i.e. graphing strain energy as a function of crack extension. This requires knowledge of the crack tip position as a function of applied load.

Nomenclature

a	crack length
a', b', c', d'	four parameters key curve fitting coefficients
a_0	initial crack length
A_{el}	elastic part of the potential energy of a loaded body
a_f	final crack length
$a_{f,m}$	measured final crack length
$a_{f,p}$	predicted final crack length
a_p	crack length of a sharp-notched specimen
A_{pl}	plastic part of the potential energy of a loaded body
b	crack ligament length
B	specimen thickness
b_b	crack ligament length of a blunt-notched specimen
b_p	crack ligament length of a sharp-notched specimen
C_0	initial specimen compliance
D	cylindrical specimen diameter
G	crack geometry function
H	material deformation function
J	J-Integral
J_0	J-Integral from total fracture energy
$J_{0.2}$	technological fracture initiation parameter
J_c	J-Integral value at fracture initiation
J_i	fracture initiation parameter
J_{IC}	critical fracture initiation parameter
J_{IQ}	fracture initiation parameter
J_{Spb}	J-Integral value at initiation of ductile tearing
k	geometry coefficient for blunting behavior
K_{IC}	critical stress intensity factor
L	cylindrical specimen height
M	bending moment
m	fitting coefficient
P	load
P_b	load of a blunt-notched specimen
P_{max}	maximum load in P–v record
P_N	normalized load
P_p	load of sharp-notched specimen
P_{tan}	tangent point in the P_N–v curve
S	span length
S_{ij}	Load Separation parameter for non-growing cracks
S_{pb}	Load Separation parameter
U	potential energy of a loaded body
v	displacement
v_{SBZ}	crack growth onset displacement
W	specimen width
Δa	crack extension
Δa_b	crack extension due to blunting
δ	crack opening displacement
η	η factor
η_{el}	elastic η factor
η_{pl}	plastic η factor
θ	rotation angle due to the presence of a crack
σ_y	yield stress

R-curves are usually constructed by using the multiple-specimen technique first developed by Landes and Begley for metals testing [17] and widely used for polymers [18–27]. Accordingly, an ESIS TC4 protocol and ASTM standard have been already developed [5,6]. It implies testing a set of nominally identical specimens loaded to different displacements such that different amount of stable crack growth occurs. Since many samples are required for a single data point, in some specific cases, it may result too time consuming, expensive, not practical when material is limited or very difficult to apply like in aggressive environments or under dynamic loading conditions. Hence, several attempts have been made in the past to infer crack extension directly from the experimentally measured load–displacement record [28,29].

The alternative expressions of J derived from limit load analysis (Eqs. (2 and 3)) have implicit the so-called Load Separation Property. This latter property assumes that the load in test measurements of specimens of the same material, geometry and constraint can be well represented as a product of two separate functions, namely a crack geometry function, $G(a)$, and a material deformation function, $H(v)$ [30]. It can be mathematically expressed in the following condensed form:

$$P(a, v) = G(a)H(v) \tag{4}$$

The separable form proposed by Eqs. (2) and (3) to represent the load generated a new factor, η, which relates the work done per unit pre-cracked ligament area in the loading of a cracked body to the *J-Integral*.

Novel methods capable of inferring *J–R* curves directly from load-line displacement records were developed based on the validity of Load Separation Property: Load Separation and Normalization methods. These single specimen methods have the appealing feature of not requiring any automatic crack growth measuring equipments.

The Normalization method infers crack extension by the construction of the material deformation function or Material Key Curve [7,31–34]. The Key Curve uniquely relates load, displacement and crack length by a separable multiplicative function, which allows constructing the material *J–R* curve. Specific literature reports successful examples of determination of *J–R* curves for different materials, including ductile metals, ceramic composites and ductile polymeric systems [35–56].

Load Separation method was originally proposed to experimentally find the η_{pl} factor in pre-cracked specimens [30]. Lately, it was extended to predict the growing crack length in pre-cracked specimens [32,40,43,56–61] and to determine the crack initiation growth parameter J_{IC}, independently of the construction of the *J–R* curve [30,32,46,17,50,62,63].

Load Separation method, also known as S_{pb} method, infers crack length growth by the comparison of load–displacement records between one stationary crack and one growing crack specimens [40,56,59–62]. Traditionally, these methods make use of the separability property in the plastic region to infer crack advance [30,31,33,34,64,65]. The elastic region is intrinsically separable and in the case of fracture of metals can be perfectly described by K_{IC} [66]. Young modulus of steel is known, and instantaneous compliance may be easily calculated from K_{IC} formula according to the popular ASTM standard [66].

Conversely, to obtain the plastic displacement component from the total displacement in polymers is not so simple. The difficulty faces when trying to fit the initial compliance with a linear function in order to define the first point of plastic displacement due to the uncertainties in Young modulus values [50,59,67]. Hale and Ramsteiner [5] stated that total fracture energy J formula (Eq. (2)) is the most appropriate for multiple-specimen testing of polymers [6] since it avoids the need to partition the area U under load displacement record into elastic and plastic components. They demonstrated that over the allowable a/W range, the formula is virtually identical to those which partition U (Eq. (3)).

This paper investigates the validity of Load Separation Property in load-line range displacement records of ductile polymers. Load Separation and Normalization methods are used to infer the *J*–R curve based on total fracture energy without distinguishing between elastic and plastic displacement components [5]. Several features of the approaches are discussed like: suitability of functional forms, influence of blunting assumption, calibration points and general limitations to their application. To this aim six tough commercial polymers are assayed.

This work also provides a deep revision of the use of the Load Separation and Normalization methods in the characterization of fracture behavior of ductile polymeric systems. Former works and corresponding references are summarized in Tables 1 and 2. Table 1 is concerned with the application of Load Separation concept while Table 2 reports the application of Normalization method to infer *J–R* curves.

2. Materials, specimens and experimental details

Six commercial grade tough polymers were investigated: three rubber-modified glassy ductile polymers and three semicrystalline polymers. High impact rubber-modified polystyrene Innova 4600 Petrobras (HIPS), Acrylonitrile butadyene styrene HI-121H, LG Chem (ABS), and Rubber-modified polymethylmetacrylate Altuglas EI50 (RT-PMMA) were kindly provided in the form of pellets by Petrobras, A.Z. Chaitas SACIF and Atofina, respectively. Pellets were dried and then compression molded to obtain flat plates for subsequent fracture characterization. Rectangular bars were cut from the plaques and machined to reach specimen final dimensions. Ultrahigh molecular weight polyethylene GUR1050, Chirulen, Poly Hi Solidur, Germany (UHMWPE), was received in the form of thick extruded plaques. RT-Nylon Latamid 6 EO02 (RT-Nylon) was kindly supplied in the form of injection molded bars by Lati Thermoplastics, Italy. RT-Nylon samples were dried during 96 hs at 80 °C under vacuum before testing. Propylene Impact Block Copolymer Hifax BA 238 G9 (PPc) was kindly provided in the form of pellets by Basell Polyolefins and processed by injection molding to obtain the test pieces.

Two types of specimens were used in the fracture experiments: Sharp and Blunt single edge notched bending specimens, *SE*(*B*). Sharp notches were introduced using a Notchvis Ceast machine with a sharp fly cutter (tip radius less than 12 μm) to reach a crack-to-depth ratio (a/W) equal to 0.5. In order to prevent heating while machining, specimens were cooled with fresh compressed air during operation.

Sets of blunt notched specimens were prepared by drilling a hole of 2 mm at the tip of a machined notch to give crack-to-depth ratios (a/W) varying from 0.5 to 0.8. In every case thickness to depth ratio (B/W) and span to depth ratio (S/W) were always kept equal to 0.5 and 4, respectively. The actual B values for each material are given in Table 1.

Mechanical characterization was carried out using an Instron 4467 testing machine equipped with automatic acquisition data facilities at room temperature. HIPS, ABS, RT-PMMA, PPc and RT-Nylon specimens were loaded in three point bending

Table 1
Summary of former publications concerned with the application of Load Separation method in polymeric materials.

Material	Loading configuration and test conditions			Paper goals and Comments	Ref.
	v (mm/min)	Specimen type	Specimen dimension (mm)		
ABS-CM	1	SE(B) - Pr	B = 7	To prove explicitly load separation in stationary and growing crack records. Verification of the theoretical η_{p1} value.	[47]
MIPS-CM HIPS-CM PPH-CM-A90 PPH-CM-A150	2 2 1 1	SE(B) - Pr SE(B) - Pr SE(B) – Pr - SG SE(B) – Pr – SG	-	To prove explicitly load separation in stationary crack records. Verification of the theoretical η_{p1} value. Determination of J_{Spb}	[48]
HDPE-EM	2	AS- NPr- SG	B × W × L = 5 × 13 × 50	To prove explicitly load separation in stationary crack records. Calibration of η_{p1} value for arc shaped side grooved specimens.	[51]
EPBC-IM	1	SE(B) – Pr	3	Influence of blunting line assumption (k = 1, 2, 4) Comparison between *J-R* S_{pb} and Normalization methods with multispecimen technique. Support Normalization method and theoretical blunting assumption.	[56]
ABS-CM MIPS-CM PPH-CM-A90	-	SE(B) – Pr SE(B) – Pr SE(B) - Pr- SG	-	Verification of the theoretical η_{p1} value.	[59]
ABS-CM	60000	SE(B) - Pr	6	Determination of *J-R* curves via *Spb* in the plastic displacement range using one and two calibration points.	[60]
PPBC-EM	60000	SE(B) – Pr	6	Methodology cannot be applied for PPBC since *J*-controlled conditions were not achieved. Materials performance.	
PPH-IM	1	SE(B) - Pr	9	To prove explicitly load separation in stationary crack records. Verification of the theoretical η_{p1} value. Determination of J_{Spb} Influence of including or not final point during calibration. Influence of the reference stationary record adopted. Materials performance.	[61]
PP-IM EPBC-IM	1 1	SE(B) – NPr - SG SE(B) – NPr - SG	B × W × L = 6 × 18 × 105 6 × 24 × 105	To prove explicitly load separation in stationary crack records. Verification of the theoretical η_{p1} value. Determination of J_{Spb}. Influence of the reference stationary record adopted. Influence of including 2 or 3 calibration points.	[62]
RT-PA66	0.5- 600	SE(B) – NPr	B × W × L = 4 × 10 × 80	To prove explicitly load separation in stationary and growing crack records. Exploration of J_{spb} validity as an initiation parameter. Influence of the reference stationary record adopted.	[63]
PP-IM PPBC-IM (neat and filled with $Mg(OH)_2$)	1	SE(B) – Pr	B = 6.35	To prove explicitly load separation in stationary crack records.	[68]
PC-EM	1.27	CT - NPr	B = 25.4 6 3	To prove explicitly load separation in stationary crack records.	[69]

Table 2
Summary of former publications concerned with the application of Normalization method in polymeric materials.

Material	Loading configuration and test conditions			Key curve function and blunting assumption	Calibration points	SBZ	Paper goals and Comments	Ref.
	Test rate (mm/min)	Specimen type	Sample Dimension (mm)					
ABS - CM	2	SE(B) – Pr	-	Power law Without blunting	*Two:* *i)* a_f from fracture surface *ii)* a_0 from fracture surface	S_{pb}	Development of methodology. *J-R* comparison with multi-specimen technique.	[46]
MIPS - CM HIPS - CM	2 2	SE(B)-Pr SE(B)-Pr	-	Plastic displacement. Power law	*Two:* *i)* a_f from fracture surface	S_{pb}	Development of methodology. *J-R* comparison with multi-specimen technique.	[48]
PPH- CM - A90 PPH- CM - A150	1 1	SE(B)-Pr-SG SE(B)-Pr-SG		Theoretical Blunting (k = 2)	*ii)* initial points from blunting line			
PVC - EM	0.1 - 50	CT	B × W = 10 × 40	Plastic displacement.	*Three:*	0.2 mm	Development of methodology.	[49]
		NPr		LMN	*i)* a_f from fracture surface		*J-R* comparison with multi-specimen technique.	
				Theoretical Blunting (k = 2)	*ii)* initial points from blunting line *iii)* intermediate points from limit load analysis			
HIPS – CM MIPS - CM ABS - CM	2 2 2	SE(B)-Pr SE(B)-Pr SE(B)-Pr	-	Plastic displacement. Power law LMN	*Two:* *i)* a_f from fracture surface *ii)* initial points from blunting line	S_{pb}	Development of methodology. Comparison of functional forms. *J-R* comparison with multi-specimen technique.	[50]
RMPMMA - CM	1	SE(B)-Pr		Combined power law-straight line.	P_L form limit load analysis for LMN		Support Power law	
PPH - CM- A 150	1	SE(B)-Pr-SG		Theoretical Blunting (k = 2)				
MDPE-CM	1	SE(B)-Pr						
HDPE - EM	2	AS-NPr-SG	B × W × L = 5 × 13 × 50	Plastic displacement.	*Two:*	S_{pb}	Development of methodology.	[51]
				Power law	*i)* a_f from fracture surface		*J-R* comparison with multi-specimen technique.	
				Theoretical Blunting (k = 2)	*ii)* initial points from blunting line			
PTFE PEEK PCTFE PCTFE- PVDF blend (75/25wt.%)	1500	-	-	Plastic displacement. Power law Theoretical Blunting (k = 2)	*Two:* *i)* a_f from fracture surface *ii)* initial points from blunting line	P_{max}	Materials performance	[53]
HIPS-CM (reinforced with 10 and 25wt. % sisal fibers)	1	SE(B) – Pr	B = 6	Plastic displacement. Theoretical Blunting (k = 2)	*Two:* *i)* a_f from fracture surface *ii)* initial points from blunting line	P_{tan}	Materials performance	[54]

UHMWPE (neat, cross-linked, sterilized) CM and EM	0.85	SE(B)-Pr	B = 20	Plastic displacement. LMN Power law Theoretical Blunting (k = 2), Blunting (k = 4), Blunting (k = 8).	*Three:* *i)* a_f from fracture surface *ii)* initial points from blunting line *iii)* intermediate calibration points.	S_{pb}	Development of methodology. *J-R* comparison with multi-specimen technique. Support Power law, being less dependent on blunting assumption than LMN. Support k = 4 for blunting behavior.	[55]
EPBC-I	1	SE(B)-NPr	B × W × L = 3 × 20 × 88	Plastic displacement. LMN Theoretical Blunting (k = 2), Blunting (k = 1), Blunting (k = 4).	*Two:* *i)* a_f from fracture surface *ii)* initial points from blunting line	P_{tan}	Evaluation of Normalization vs S_{pb} methods performance.	[56]
PPBC – IM - A110	1	SE(B)-Pr	B = 6.35	Plastic displacement. LMN and Power law Theoretical Blunting (k = 2), Blunting (k = 4), without blunting.	*Two:* *i)* a_f from fracture surface *ii)* initial points from blunting line LMN determination by least squares from initial points and final point.	S_{pb}	*J-R* comparison with multi-specimen technique. Comparison of Key Curve functional forms. Influence of blunting assumption. Support k = 4 and Power law	[67]
PPBC- IM- A110 PPH – IM - A110 (filled with Mg $(OH)_2$ different contents)	1 1	SE(B)-Pr	B = 12.7	Plastic displacement. Power law Theoretical Blunting (k = 2), Blunting (k = 4), without blunting.	*Two:* *i)* a_f from fracture surface *ii)* initial points from blunting line	S_{pb}	Development of methodology. Influence of blunting assumption. *J-R* comparison with multi-specimen technique.	[68]
PC - EM	1.27	CT NPr	B × W = 25.4 × 50.8 6 × 50.8 3 × 50.8	Plastic displacement. LMN Theoretical Blunting (k = 2)	*Three:* *i)* a_f from fracture surface *ii)* initial points from blunting line *iii)* intermediate points from limit load analysis	P_{max}	Development of methodology. *J-R* comparison with multi-specimen technique.	[69]
RTN66 – IM RTAN – IM	1 1	SE(B) - Pr	B = 12.7, 6.4, 3.2	Plastic displacement. Power law Theoretical Blunting (k = 2)	*Three:* *i)* a_f from fracture surface *ii)* initial points from blunting line *iii)* intermediate points from limit load analysis	P_{max}	Development of methodology. *J-R* comparison with multi-specimen technique.	[70]

(*continued on next page*)

Table 2 (*continued*)

Material	Loading configuration and test conditions			Key curve function and blunting assumption	Calibration points	SBZ	Paper goals and Comments	Ref.
	Test rate (mm/min)	Specimen type	Sample Dimension (mm)					
PTFE	0.025-24000	CT-Pr	B = 14	Plastic displacement. 4 Parameter Analytical function Theoretical Blunting (k = 2)	*Two:* *i)* a_f from fracture surface *ii)* initial points from blunting line	P_{tan} P_{max}	Materials performance	[71]
PTFE (filled with 25% Al)	$1.5x10^{-2}$ - 21000	CT-NPr	B × W = 25.4 × 39	Plastic displacement. 4 Parameter Analytical function Theoretical Blunting (k = 2)	*Two:* *i)* a_f from fracture surface *ii)* initial points from blunting line	P_{tan}	Materials performance	[72]
RTN66-IM	1000	SE(B) -NPr	B × W × L = 4 × 10 × 80	Plastic displacement. Power law Theoretical Blunting (k = 2)	*Two:* *i)* a_f from fracture surface (stop block) *ii)* initial points from blunting line	S_{pb}	*J-R* comparison with multi-specimen technique.	[73]

configuration at a crosshead speed of 2 mm/min. Due to their inherent ductility PPc and UHMWPE samples were tested at 5 mm/min and at 50 mm/min respectively [5,55,74]. Yield stress, σ_y, of ABS, RT-PMMA, PPc, UHMWPE and RT-Nylon specimens were determined from uniaxial tensile tests carried out on type IV dumb-bell shaped specimens [75]. Yield stress of HIPS was determined in compression using cylindrical specimens having and aspect ratio (L/D) of 1.5 since under tensile loading it broke without yielding. σ_y values were determined in the way conventionally accepted for polymers: as the point where the force–elongation curve shows a local maximum [76]. The crosshead speed for HIPS, ABS, RT-PMMA, and RT-Nylon specimens was 2 mm/min, for PPc was 5 mm/min and for UHMWPE was 50 mm/min. The material's yield stress and plate thickness values are reported in Table 1.

In order to generate suitable load–displacement records for the application of Normalization and S_{pb} methods sharp specimens were bended up to a certain prefixed displacement level after the maximum load allowing the crack to grow to a length of about 10% of the initial remaining ligament. After unloading the actual initial and final crack lengths, a_0 and a_f, were physically determined. To avoid artifacts in the determination of crack growth, tested specimens were sectioned at the midplane along to their longitudinal axis. One of the cut pieces was polished to reveal crack growth, which was determined from microscopy observation of the side view, for all materials but PPc. For the latter, tested specimens were cryogenically broken under impact conditions and crack growth amount was determined from the fracture surface simply because this copolymer is black colored. Blunt notched specimens were used to simulate stationary records due to the absent of large tensile stresses. They were loaded up to sufficiently large displacement levels or up to the instability point in which the assumption of stationary behavior was violated.

Additionally, a set of 10–15 identical sharp notched specimens were loaded up to different displacement levels allowing the crack to reach different crack growth lengths and fully unloaded before complete fracture to construct benchmark multiple-specimen J–R curves for each material.

3. Data reduction methods

3.1. Load Separation Property analysis

The Load Separation Property allows the expression of the load, P, applied to a notched body as a product of two independent functions: a geometry dependant function (including crack length), and another function dependent on material deformation properties. Similarly to the developments available in literature, assuming the validity of Load Separation in the plastic displacement regime [31,77] we can speculate that the load can be represented as a product of two functions: a crack geometry function, G, and a material deformation function, H as follows:

$$P = G\left(\frac{b}{W}\right)H\left(\frac{v}{W}\right) \tag{5}$$

$$b = W - a \tag{6}$$

where v represents the displacement, W is the characteristic length of the body, a is the crack length and b is the ligament length. A separation parameter, S_{ij}, is defined as the load ratio of two stationary crack specimens of the same size and material, with different ligament lengths b_i and b_j at a fixed value of displacement:

$$S_{ij} = \left.\frac{P(b_i)}{P(b_j)}\right|_v \tag{7}$$

where $P(b_i)$ represents the applied load to a specimen with a crack length, a_i and $P(b_j)$ represents the applied load to another specimen with crack length, a_j. Both a_i and a_j remain constant during the test. Substituting Eq. (7) into Eq. (5) yields

$$S_{ij} = \left.\frac{G(\frac{b_i}{W})H(\frac{v}{W})}{G(\frac{bj}{W})H(\frac{v}{W})}\right|_v \tag{8}$$

and then:

$$S_{ij} = \left.\frac{G\left(\frac{b_i}{W}\right)}{G\left(\frac{bj}{W}\right)}\right|_v \tag{9}$$

Since the geometry function is constant for stationary crack experiments, if S_{ij} takes a constant value over the whole domain of displacement then the load can be represented by a separable form for this set of material, geometry, constraint and test conditions (Eq. (9)). Hence, by computing the ratio of loads (Eq. (7)) for a set of blunt notched samples, Load Separation hypothesis can be easily checked.

From the separable form of the load, the η parameter can be evaluated from the following expression:

$$\eta = \frac{\left(\frac{b}{W}\right)}{G\left(\frac{b}{W}\right)} \cdot \frac{dG\left(\frac{b}{W}\right)}{d\left(\frac{b}{W}\right)} \tag{10}$$

The $G(b/W)$ function can be constructed from experimentally determined S_{ij} values, as:

$$S_{ij}\left(\frac{b_i}{W}\right) = C_1 \cdot G\left(\frac{b_i}{W}\right) \quad \text{for constant } \frac{b_j}{W} \tag{11}$$

where C_1 is a constant equal to $1/G(b_j/W)$. If a power law fits accurately the geometry function:

$$G\left(\frac{b}{W}\right) = \left(\frac{b}{W}\right)^{\eta} \tag{12}$$

then η can be calculated from Eqs. (11) and (12).

3.2. Multiple specimen procedure

Benchmark J–resistance curves were determined by the traditional multiple-specimen technique, originally developed for metals [78] and then applied to polymers displaying flat or gently rising R-curves [5,6]. It consists in loading a series of identical specimens to various sub-critical displacements, producing different amounts of crack extension, Δa. The value of J for each specimen was calculated from the total fracture energy and crack growth corrected area. For $SE(B)$ specimen:

$$J_0 = \frac{2U}{B(W - a_0)} \tag{13}$$

$$J = J_0\left[1 - \frac{0.5\Delta a}{W - a_0}\right] \tag{14}$$

being $\Delta a = a - a_0$.

J–R curves were then fitted following two different procedures recommended by the metal standard ASTM E813-89 [17], and ASTM D6068-96 [79] and ESIS Protocol [5]. The first procedure which was extensively used at the early beginning of J-testing of polymers proposes a bilinear approximation of the J–R curve [8,19,21,80]. The first line, called the blunting line represents the apparent crack growth due to blunting of the crack tip before crack propagation by ductile tearing. It has the analytical expression:

$$J = k\sigma_y \Delta a \tag{15}$$

where σ_Y is the tensile yield stress, and k is a geometry coefficient. Assuming that the crack tip is semicircular, apparent crack growth due to blunting, Δa_b, is half the crack opening displacement, δ, and hence k equals 2. The second line is fitted asymptomatically to experimental stable crack growth data. A physical critical fracture initiation value J_{IQ} (J_{IC} in plane strain) is taken to be the point where the two lines intersected. Latter revisions to the methods led to the generation of the new procedure described by ASTM D6068-96 and ESIS Protocol. $J - \Delta a$ data points are fitted to a power law:

$$J = C\Delta a^n \tag{16}$$

Since for many materials measuring crack growth has proved not to be trivial, a pseudo-fracture initiation parameter called $J_{0.2}$ is determined at 0.2 mm of total crack growth avoiding measuring an initiation value as done in former versions.

It is well known that ductile fracture, starting from a pre-existing crack, may be preceded by the following four phases: blunting of the crack followed by the initiation of crack growth, which then evolutes into stable crack propagation and ends with unstable and rapid crack propagation. The qualitative and the quantitative evolution of the previously mentioned phases are dependent on the properties of the materials and the geometry of the specimens, as well as on the geometry of the crack [81]. Despite, the universal validity of theoretical blunting line expression for polymers have been questioned since long time [68,82] blunting should be assumed to be semi-circular (Eq. (15) with k equals 2) for predictive purposes [69,70,83].

Through this paper the crack tip constraint factor, k, was taken to be 2 for all of the polymer assessed except for UHMWPE in which a value of 4 is adopted *a priori* according to the value first proposed by Pascaud et al. [74] and confirmed by further investigations [55,84,85].

3.3. Load Separation method, S_{pb}

Another separation parameter, S_{pb}, may be defined by dividing the load of a sharp-notched specimen, P_p, by the load of a blunt-notched specimen, P_b, at constant displacement as follows:

$$S_{pb} = \left.\frac{P_p(b_p, v)}{P_b(b_b, v)}\right|_v \tag{17}$$

where b_p and b_b are the crack ligament lengths of the sharp-notched and blunt-notched specimens, respectively.

Taking into account that blunt notched specimens behave as stationary crack specimens [73] while sharp notched specimens behave as growing crack specimens, the following analysis can be performed. Provided that the separation property holds, the separation parameter would get a constant value as long as the sharp crack remains stationary or would slightly decrease as long as non-negligible crack tip blunting occurs in the sharp-notched specimen [40,60,68]. Conversely, a steep drop of S_{pb} trend identifies the displacement value in correspondence with the onset of crack extension by ductile tearing.

Introducing Eq. (5) in Eq. (17), the S_{pb} parameter at constant displacement can be rewritten as:

$$S_{pb} = \left. \frac{G_p\left(\frac{b_p}{W}\right) \cdot H\left(\frac{v}{W}\right)}{G_b\left(\frac{b_b}{W}\right) \cdot H\left(\frac{v}{W}\right)} \right|_v \tag{18}$$

As both specimens have the same geometry, i.e. same W, B, and S/W, and are made of the same material, the deformation functions ratio in Eq. (18) is equal to identity when they are determined at constant displacement. Then Eq. (18) can also be expressed by:

$$S_{pb} = \left. \frac{G_p\left(\frac{b_p}{W}\right)}{G_b\left(\frac{b_b}{W}\right)} \right|_v \tag{19}$$

Adopting the common power law function format for the geometry function, $G(b/W)$, given in Eq. (12) [30,32,70,86]:

$$G\left(\frac{b}{W}\right) = \left(\frac{b}{W}\right)^m \tag{20}$$

another expression for the S_{pb} parameter can be derived by introducing Eq. (20) into Eq. (19):

$$S_{pb} = \frac{\left(\frac{b_p}{W}\right)^m}{\left(\frac{b_b}{W}\right)^m} = \left. \left(\frac{b_p}{b_b}\right)^m \right|_v \tag{21}$$

From Eq. (21), it directly emerges that the crack ligament length of the sharp-notched specimen, b_p, can be expressed as:

$$b_p = b_b \cdot \left(S_{pb}\big|_v\right)^{\frac{1}{m}} \tag{22}$$

and the crack length, a_p is then

$$a_p = W - b_b \cdot \left(S_{pb}\big|_v\right)^{\frac{1}{m}} \tag{23}$$

Rigorously Eq. (22) can be fitted by using only one calibration point. Obviously, fitting confidence is improved when more than one calibration points are included in calculations. Hence, the m parameter was determined fitting Eq. (22) by minimum least squares, following two procedures according to the calibration points utilized:

Procedure I. Considering two calibration points

(i) (b_{p0}, S_{pb0}), the initiation of ductile tearing.
(ii) (b_{pfi}, S_{pbf}), the final point.

The first point (i) is determined from the first part of the S_{pb}–displacement plot where only crack growth due to blunting is assumed to occur in the sharp-notched specimen. The crack length at the initiation of ductile tearing is estimated from the initial crack length, a_0, plus the crack growth due to blunting. So that the crack ligament length at the initial of ductile tearing, b_{p0}, is estimated as:

$$b_{p0} = W - \left(a_0 + \frac{J_0}{k\sigma_y}\right) \tag{24}$$

where σ_y is the yield stress and J_0 is given by Eq. (13).

The second point (ii) is taken from the last point of the S_{pb}–v plot and the final ligament length, b_{pf}.

Procedure II. Considering one calibration point

(i) (b_{p0}, S_{pb0}), the initiation of ductile tearing.

This procedure has been proved to be very useful when final point is not easy to determine like in impact fracture testing [60].

Knowing the m parameter, the crack length, a_p, at every point of the load displacement record can then be inferred from Eq. (23).

Material fracture toughness is defined near the initiation of stable crack growth. The precise point at which crack growth begins is usually ill-defined. It was suggested by Sharobeam and Landes [30] that independently of the construction of the J–R curve, an initiation fracture toughness parameter, J_{Spb}, taken as the J value at initiation of ductile tearing can be directly determined in coincidence with the point (i). This criterion provides in principle a viable and simple test technique to define fracture initiation. Nevertheless, it has been tried to polymers only in few opportunities without any deep analysis [60,68] since recently, when Baldi et al. provided a very serious investigation upon this methodology [63].

3.4. Normalization Data Reduction procedure

Normalization Method proposes an individual normalized calibration curve, in which load, displacement, and crack length can be functionally related for each specimen in reference to load versus displacement record only. This calibration curve is then used to determine the instantaneous crack length in conjunction with the load and displacement test data. The change in crack length as fracture progresses is inferred by comparing the measured and normalized load versus load-line displacement records with an analytical normalization function fit to initial and final load, displacement, crack length data [42]. Different calibration functions have been proposed so far, including power-law function [35,87], combined function of power law and straight line [36], and three-parameter LMN function [37,38]. The suitability of these functional forms in capturing deformation characteristics of different ductile polymers have already been discussed in literature [50,67].

Specific scientific community assented to adopt the simplified four parameter version of LMN function as the most convenient option for steel testing [88]. This latter version has the inherent advantage of allowing the use of only two reference crack lengths to fit the deformation function in contrast to the previously required three points [39]. Recently, ASTM E1820-01 Normalization Reduction approach was also applied to determine J–R curves of different polymeric systems providing encouraging performance [56,72]. Though, aiming to generalize methodology and simplify future analysis, the approach used through this paper follows the method lineament proposed by ASTM E1820-01. Indeed, calculations are made using directly load-line displacement records according to Donoso and Landes suggestions [89]. They supported the idea that when load is separable, simple formats of H function could represent any type of deformation not only plastic deformation.

The procedure described in what follows makes use of the Four-parameter analytical ASTM function to represent deformation in the whole range of displacement. Conversely to Normalization Data Reduction procedures based on normalized plastic displacement, this approach is non-iterative and function parameters are determined straightforwardly.

Guide to method:

(i) Each value of the load P_i up to, but not including P_{max} , is normalized using Eq. (25) expression based on the estimated blunted crack length, a_b, by assuming theoretical blunting behavior (Eq. (15)).

$$P_{N_i} = \frac{P_i}{WB \cdot \left[\frac{W-a_{bi}}{W}\right]^{\eta}} \tag{25}$$

$$a_{bi} = a_0 + \frac{J_0}{k\sigma_y} \tag{26}$$

(ii) Normalized final point, P_{Nf}, is calculated from the load point in correspondence with maximum displacement normalized by the final measured crack extension, a_f:

$$P_{Nf} = \frac{P_f}{WB \cdot \left[\frac{W-a_f}{W}\right]^{\eta}} \tag{27}$$

(iii) In order to select data for the fitting procedure, a line from the normalized final point tangent to normalized load-total displacement curve is drawn. The purpose of drawing the tangent line [39] is to exclude points with excessive ductile tearing or subcritical crack growth in the so-called stable blunting zone, *SBZ*.

(iv) Data between tangent point and normalized final point plus data meeting condition in Eq. (28) should be excluded:

$$\frac{v_i - P_i \cdot C_0}{W} < 0.001 \tag{28}$$

where C_0 is the initial specimen compliance determined directly from the initial slope of the load-line displacement curve.

(v) The remaining data is then fitted to the following rational function:

$$P_{N_i} = \frac{a' + b'\frac{v}{W} + c'\left(\frac{v}{W}\right)^2}{d' + \frac{v}{W}} \tag{29}$$

where a', b', c', d' are the searched fitting coefficients.

(vi) Then, crack length, a, may be inferred for each load–displacement pair by equating Eq. (25) into Eq. (29).

$$\frac{P_i}{WB\cdot\left[\frac{W-a_i}{W}\right]^{\eta}}=\frac{a'+b'\frac{v}{W}+c'\left(\frac{v}{W}\right)^2}{d'+\frac{v}{W}} \tag{30}$$

(vii) When the crack lengths are determined, the J–R curve can be then calculated from the individual J-Integral values estimated via Eq. (14).

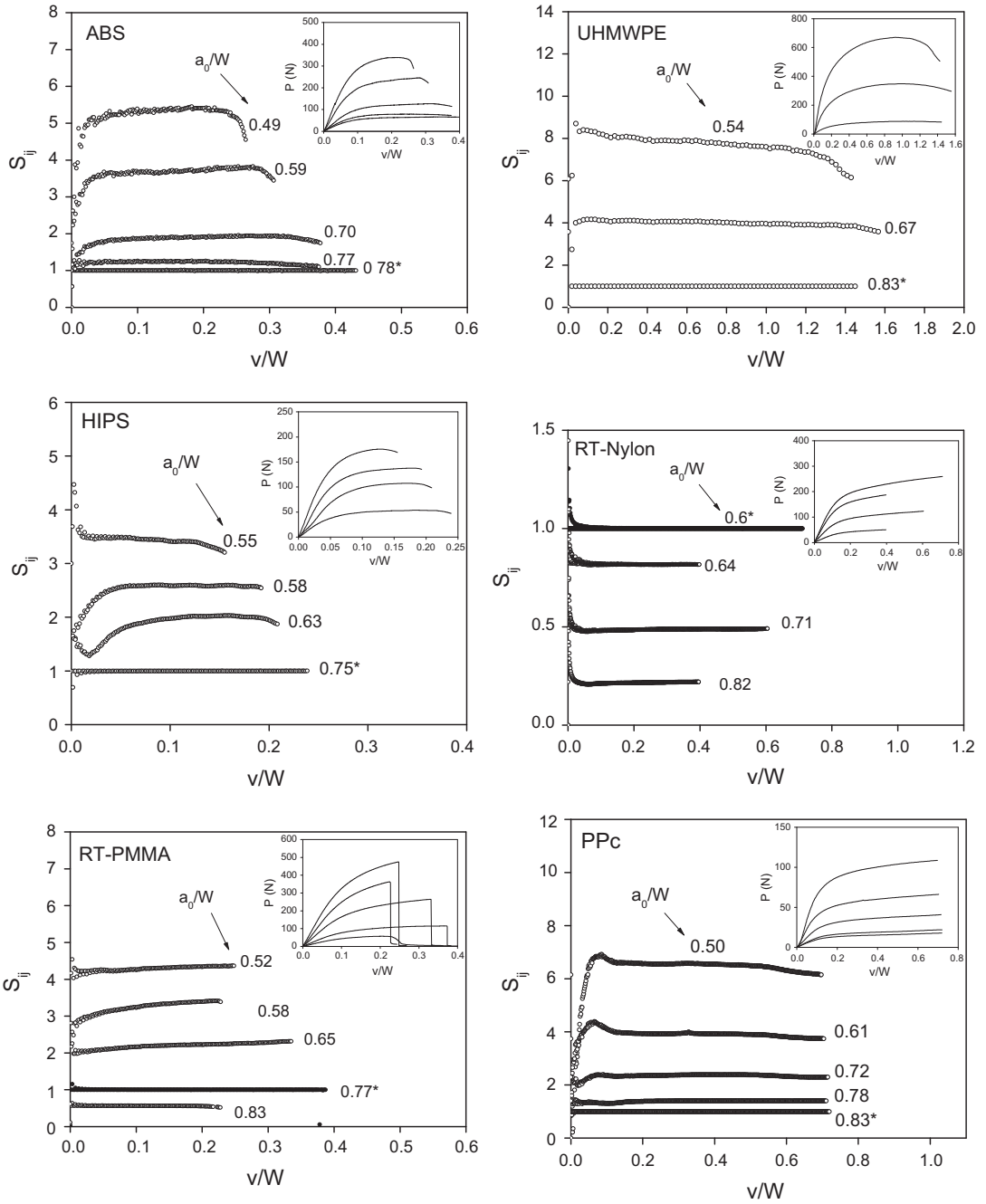

Fig. 1. S_{ij} parameter at constant displacement plotted in terms of displacement to sample width ratio. The reference record (j) used in S_{ij} calculation is indicated with an *. Plots inside correspond to the load-line curves of blunt-notched specimens.

4. Results

4.1. Load Separation Property

Fig. 1 shows the separability parameters S_{ij}, determined at constant displacement, computed from blunt load-line records (also shown in the figure). Consistently with expectations, blunt specimens behave basically stationary. Depending on material type and geometry (initial crack length), at a certain displacement level crack unstabilizes and hence, the assumption of non growing crack growth collapses. Some specimens of rubber modified glassy polymers unstabilize at low displacement levels. In particular, RT-PMMA samples were the least prone to stable propagation. Conversely, specimens of the three semicrystalline polymers remain stationary up to much higher displacement levels reminding steel behavior [32,40,48]. Deeper notches promote stable crack propagation up to larger displacement levels since these types of samples accumulate less elastic energy.

Previous investigations demonstrated the validity of Load Separation in the plastic displacement regime for several ductile polymers [43,46,48,50,56,62]. S_{ij}, remains almost constant for the whole range of total displacement except for a limited region at the beginning of displacement [32,43,56,59–61,69,90]. The breaking down of Load Separation Property at these small displacement levels implies that η is not defined within this initial region. This non-constant S_{ij} region is larger for a/W ratios far from the a/W ratio of the sample taken as the reference record. It was previously argued that S_{ij} attained a constant value in coincidence with the development a fully plastic regime [32,43,69,90]. It is believed that crack tip stresses and strains are influenced by the original blunt crack tip during the early stages of crack growth. In any case, the non-constant region resulted small in comparison with the total displacement range involved in the experiments allowing assuming that S_{ij} parameter is independent of displacement, being only a function of crack length. Therefore, the validity of Load Separation Property assumption for all of these materials has been confirmed in terms of displacement.

From S_{ij} at constant displacement values, η was estimated for each material according to the power law model (Eq. (12)) from Eq. (11). The results reported in Fig. 2 show η values varying from 1.847 to 2.05, which can be taken equal to the theoretical one for this geometry ($\eta = 2$). Deviations from the theoretical value 2 may be related to the differences in the material work hardening or simply by experimental errors. Also, previously published papers had experimentally confirmed a value close to 2 for η_{pl} for different ductile polymers [46,48,56,62,69].

4.2. Multiple specimen J–R curves

Regarding sharp notched samples, a simple analysis of load displacement traces shown in Fig. 3 reveals that all materials exhibited non linear load–displacement traces and completely stable fracture, i.e. crack growths in correspondence with the continuous increase in displacement until complete fracture. Some differences in the shape of the curves related with each material type behavior appear evident. Rubber modified glassy polymers which, have relatively low toughness and high yield stress, behaved linear up to a certain load beyond they departed from linearity but the load continued to increase until reaching a well-defined maximum. In contrast, the curves displayed by semicrystalline polymers have less defined broad peaks and displacement levels are significantly larger due to the high degree of blunting displayed by these ductile materials. Typically, they have relatively high toughness and low yield stress. The pictures included in Fig. 3 confirm stable propagation in every case.

Notably, in the case of RT-PMMA, its transparency allowed us to clearly detect crack propagation onset well before maximum load was reached as indicated in Fig. 3 (RT-PMMA plot). The *J–R* curves constructed using multiple-specimen

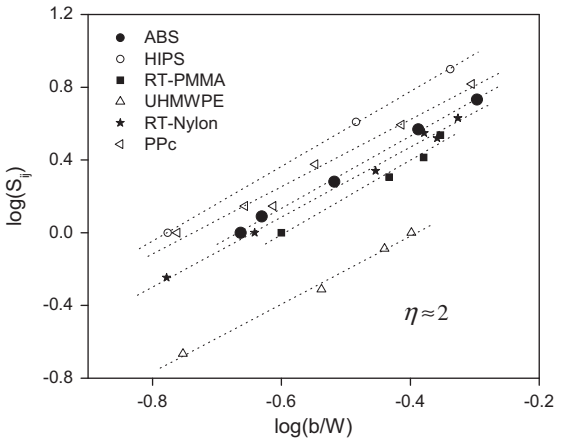

Fig. 2. Determination of η parameter from non-growing crack experiments.

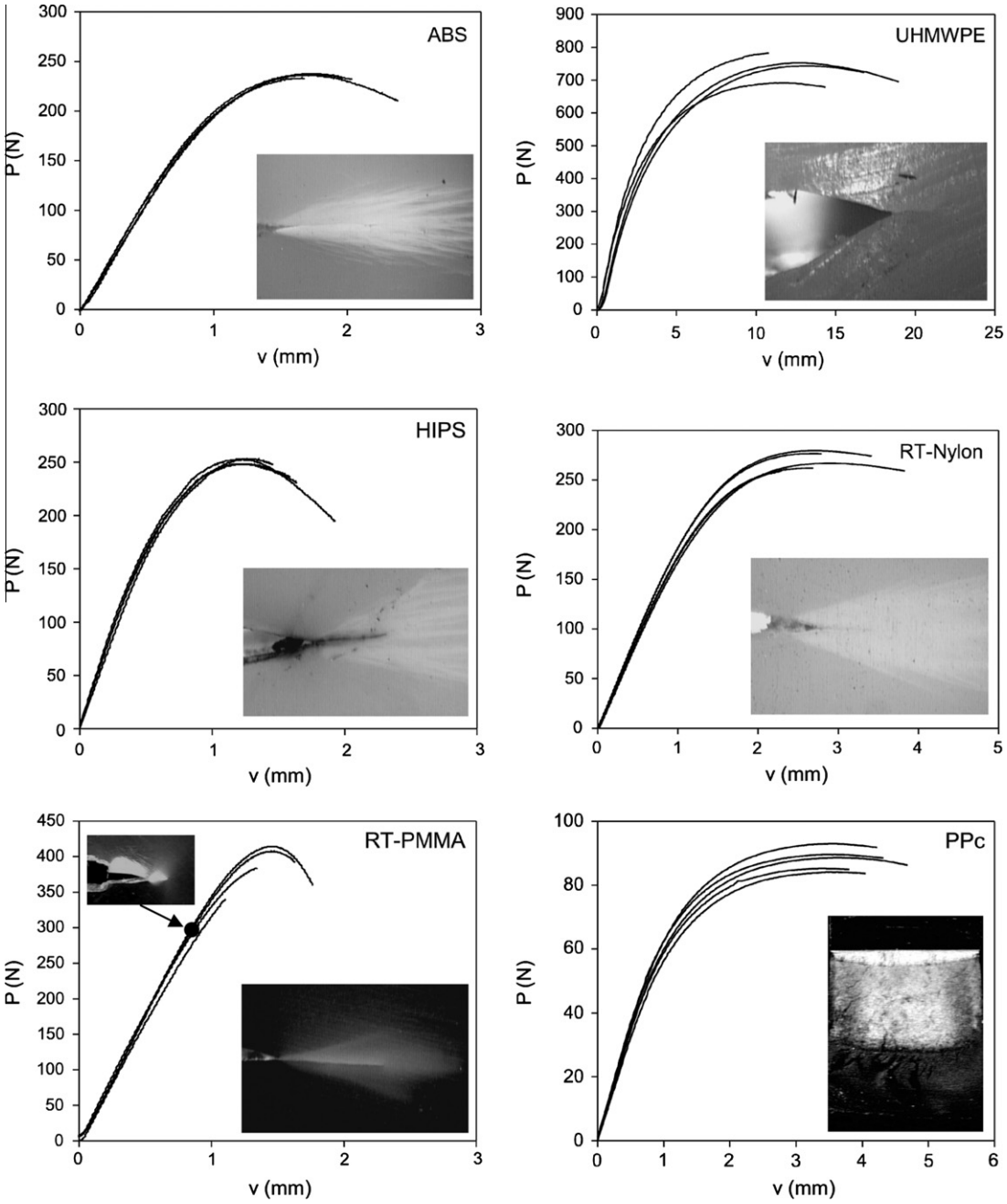

Fig. 3. Fracture experiments results: Typical load displacement curves of sharp notched specimens and macrographs used for crack growth determination (crack propagation zone in the centre of the specimen for ABS, HIPS, RT-PMMA, UHMWPE and RT-Nylon and crack front from the fracture surface for PPc). For RT-PMMA filled dot and additional macrograph indicate the optically observed fracture propagation onset.

technique are shown in Fig. 4. They exhibited the typical scatter thrown by this methodology that makes use of several theoretical identical specimens which, in real experiments display unavoidable small differences. Emerging parameters are listed in Table 3. The fact that some specific J_{IQ} data did not meet plane strain requirements, as specified in the footnote of Table 3, is not relevant in the context of the present paper. Hence, for the semicrystalline polymers the developed J–R curves may be not strictly geometry independent. Plastic processing techniques impose a severe technological limitation in the thickness of samples to be tested. Specifically, for injection molding parts meeting plane strain conditions may be sometimes a rather utopian goal.

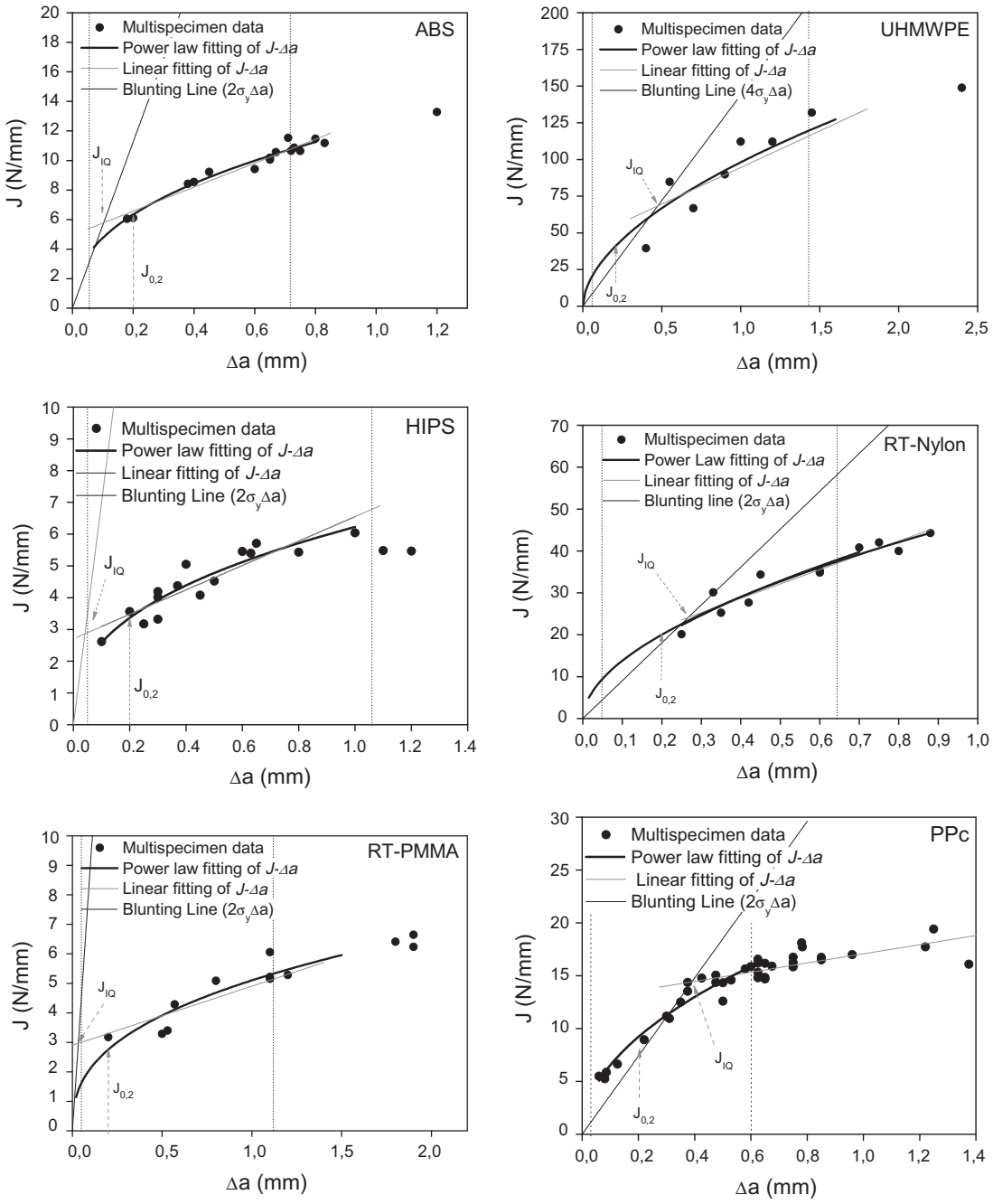

Fig. 4. Multispecimen technique results: *J–R* curves, exclusion lines, theoretical blunting line, and fracture toughness parameters (J_{IQ} and $J_{0.2}$) determination.

Our fracture experiments on UHMWPE reconfirm that blunting behavior for this material is not well described by theoretical blunting line and hence, a *k* value equal to 4 should be used [74]. For the other materials, theoretical blunting lines seem to describe pretty well the behavior before ductile tearing confirming what had been widely observed in the past [5]. Nonetheless, these findings cannot be considered a general conclusion since different trends had been reported by other authors for similar resins (see for instance in [63,82]).

PPc shows a different behavior, instead of the typical rising *J–R* curve it displays an "almost flat" R-curve, similar to the one shown by Hale et al. for HDPE at −20 °C [5]. Conversely, other propylene polymers tested in the past had shown rising *J–R* curves [56,67].

Table 3
Summary of material's parameters: Yield stress (σ_y) and Fracture Toughness (J_{IQ}, $J_{0.2}$); actual specimen thickness values (B) and plane strain size requirements (B').

Material	Yield stress σ_y (MPa)	Fracture Toughness J_{IQ} (N/mm)	$J_{0.2}$ (N/mm)	Size B (mm)	B′ [a] (mm)
ABS	28.1	5.8	6.2	7.7	5.2
HIPS	35.0	2.9	3.4	9.2	2.1
RT-PMMA	45.0	3.0	2.8	11.2	1.7
UHMWPE	36.0	68.4	40.4	12.8	47.5×
RT-Nylon	45.2	24.2	20.4	6.4	13.4×
PPc	18.2	14.4	9.3	6.4	19.8×

[a] Size requirements were evaluated from $B' > 25\, J_{IQ}/\sigma_y$ [5]. Symbol × indicates that size requirements were not met.

4.3. Load Separation method J–R curves

The S_{pb} parameters evaluated according to the definition given in Eq. (17) from load–displacement raw data are shown in Fig. 5 – *left column*. Basically, the variation of S_{pb} with displacement follows the two main patterns first pointed out by Sharobeam and Landes [30] and later confirmed in polymer testing [47,48,66,67]. At low values of displacement, at which Load Separation condition is not still fully developed, S_{pb} shows a not well defined trend. Then, the separation parameter maintains an almost constant value, i.e. non crack growing region, followed by a region showing a continuously decreasing trend of the S_{pb} parameter as the displacement increases, in coincidence with ductile tearing. The second pattern, displayed by semicrystalline polymers, shows two continuously decreasing regions characterized by different slopes. This behavior, which lacks of a constant region, is consistent with not negligible apparent crack growth due to crack tip blunting. The final decreasing S_{pb} zone in which, S_{pb} decreases with a steeper slope corresponds to the ductile tearing stage.

The displacement value corresponding to the initiation of ductile tearing, v_{SBZ}, determines the first calibration point (i) for m parameter determination (see Section 3.3, Eq. (21)). The detection of the crack growth onset, sometimes rather subjective and distressing, constitutes the main issue in this method [56–62]. Bearing in mind the mentioned difficulties, this point has been always taken through this paper in coincidence with the interception of two asymptotic lines drawn on the S_{pb} plots as shown in the Fig. 5 – *left column* denoting the slope change in S_{pb} diagrams. Once the crack growth onset point (b_{p0},S_{pb0}) was identified, the m parameter for each set of sharp and deeply blunt notched specimens was calculated following the procedures described in Section 3.3. Values arisen from *Procedure I* are listed in Table 4. As expected m parameter was very similar to the theoretical value of 2 [40]. Then, by means of Eqs. (13), (14), and (22), the crack length and the *J-Integral* values for every point of the load–displacement records were inferred (Fig. 5 – *right column*).

The reproducibility of the inferred *J–R* curves was checked by trying out two sharp notched specimens having different final crack extensions. The quality of predictions was judged by comparing inferred *J–R* curves with multi-specimen technique (Fig. 5 – *right column*); and from the relative error between the inferred final crack length, $a_{f,p}$, and the physically measured, $a_{f,m}$, values (Table 4).

Very good agreement between the *J–R* curves predicted by Load Separation method and the multiple-specimen technique was found for UHMWPE and RT-Nylon.

Less satisfactory *J–R* curves were found for rubber modified glassy polymers. In this case S_{pb} method slightly underestimates crack growth that seems to be consistent with an important subcritical crack growth not described by the theoretical blunting concept. In this type of materials toughness usually arises from coarse cavitation of the dispersed phase while the matrix remains unplasticized and still very elastic. However, the initiation of crack growth optically determined for RT-PMMA, J_i, (RT-PMMA plot in Fig. 3) appeared at load levels before to the one defined by the S_{pb} crack onset, v_{SBZ} , (RT-PMMA plot in Fig. 5) . In this type of polymers the incidence of blunting growth in total crack growth is negligible since they display relatively low toughness and high yield stresses. Indeed, similar *J–R* curves can be obtained simply applying the first version of S_{pb} method which obviates blunting growing [59]. Most of the literature related to S_{pb} method in polymers is concerned with its application to semicrystalline polyolefins [56,62] in which, this method performed in a better way rather than to rubber modified glassy polymers [91]. Despite the hard efforts done by the authors, the real reason causing S_{pb} method to work worst for rubber glassy polymers could not be identified and still remains as an open question.

The "almost flat" *R*-curve exhibited by PPc implies that a low degree of correlation between *J* values and crack growth, Δa, data points exists. In such a case S_{pb} method cannot work since different a_i values are associated with the same value of *J*. This is clearly shown in PPc plot of Fig. 5 – *right column*, where data reduction is made using four different samples leading to four different *R*-curves.

The difference between estimated and measured cracks lengths as well as the inferred *J–R* curves were practically independent on the exact determination of the ductile tearing initiation point, v_{SBZ}, and the blunt notched sample used as reference (Fig. 6a and b). The sensitivity of methodology to the accuracy in onset of ductile tearing point determination has been investigated in the past [56,59]. They concluded that negligible differences were reflected in *J–R* curves. In addition, the *J–R* curves developed using only one calibration point (*Procedure II* in Section 3.3), practically superimpose the ones constructed with two calibration points (*Procedure I* in Section 3.3) as shown in Fig. 6c).

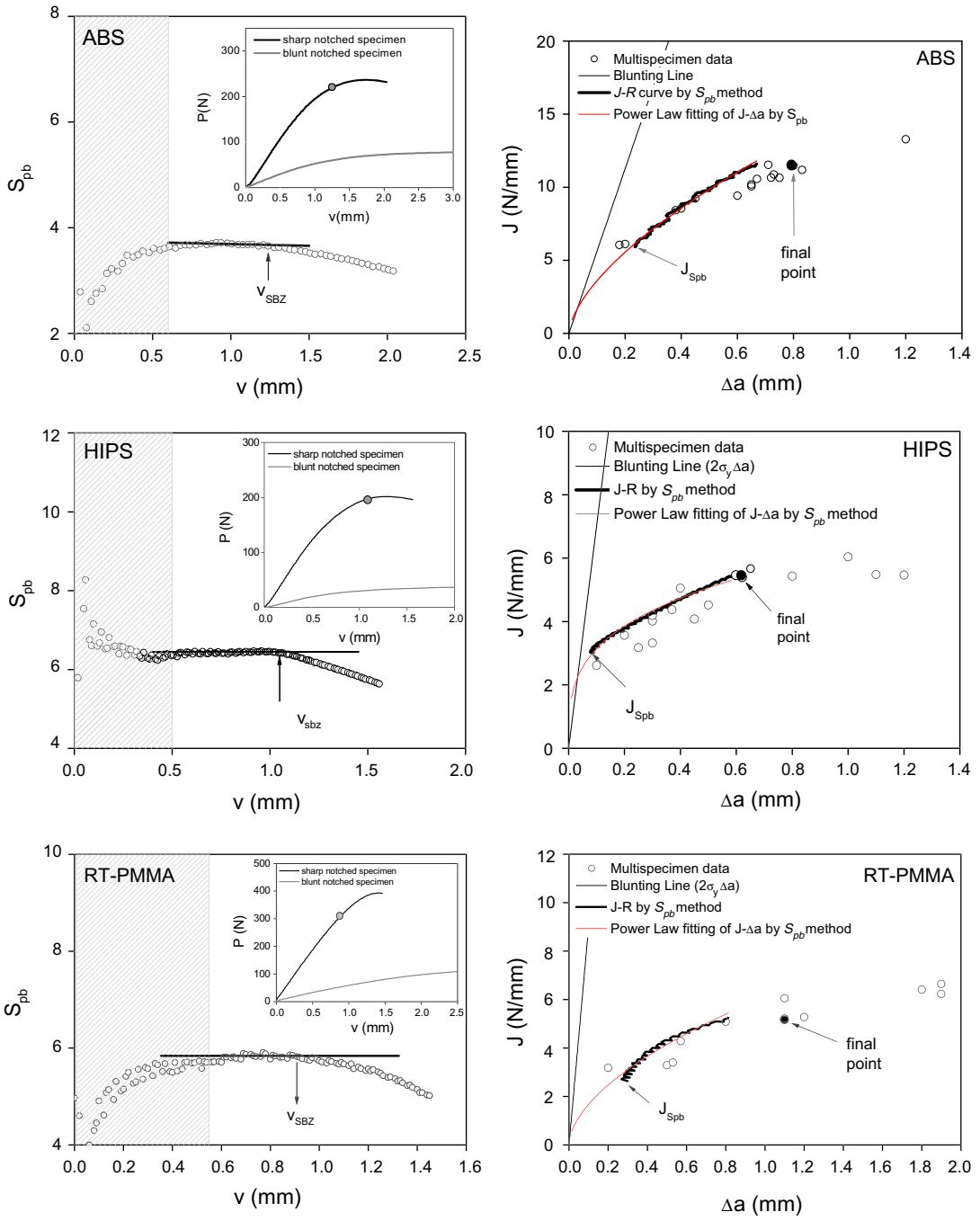

Fig. 5. S_{pb} Method results: S_{pb} parameter vs. displacement plots (*left column*), predicted *J–R* curves and J_{Spb} parameter determination (*right column*). Gray filled dot in the included *P–v* plots indicate ductile tearing initiation onset (left column). The dashed zone in S_{pb} vs. *v* plots shows the non-separable blunting region.

Although the entire *R*-curve gives a more complete description, initiation toughness provides important information about the fracture behavior of a ductile material. J_{IQ} is defined near the initiation of stable crack growth. The precise point at which crack growth begins is still a question of debate in polymers, especially for high toughness materials exhibiting low yield stress as rightly pointed out by Patel et al. [3]. Besides, Fig. 5 and Table 4 show the J_{Spb} values determined directly from fracture energy at the displacement point in coincidence with the initiation of ductile tearing from S_{pb} plots. These values resulted, indeed, very sensitive to the selected reference sample as shown in Fig. 6b). The latter analysis was carried out inspired in the recent ideas presented by Baldi et al. [63]. After a deep study, they achieved the conclusion that, unfortunately and despite the appealing of this simple approach, a unique initiation value could not be determined from the simply

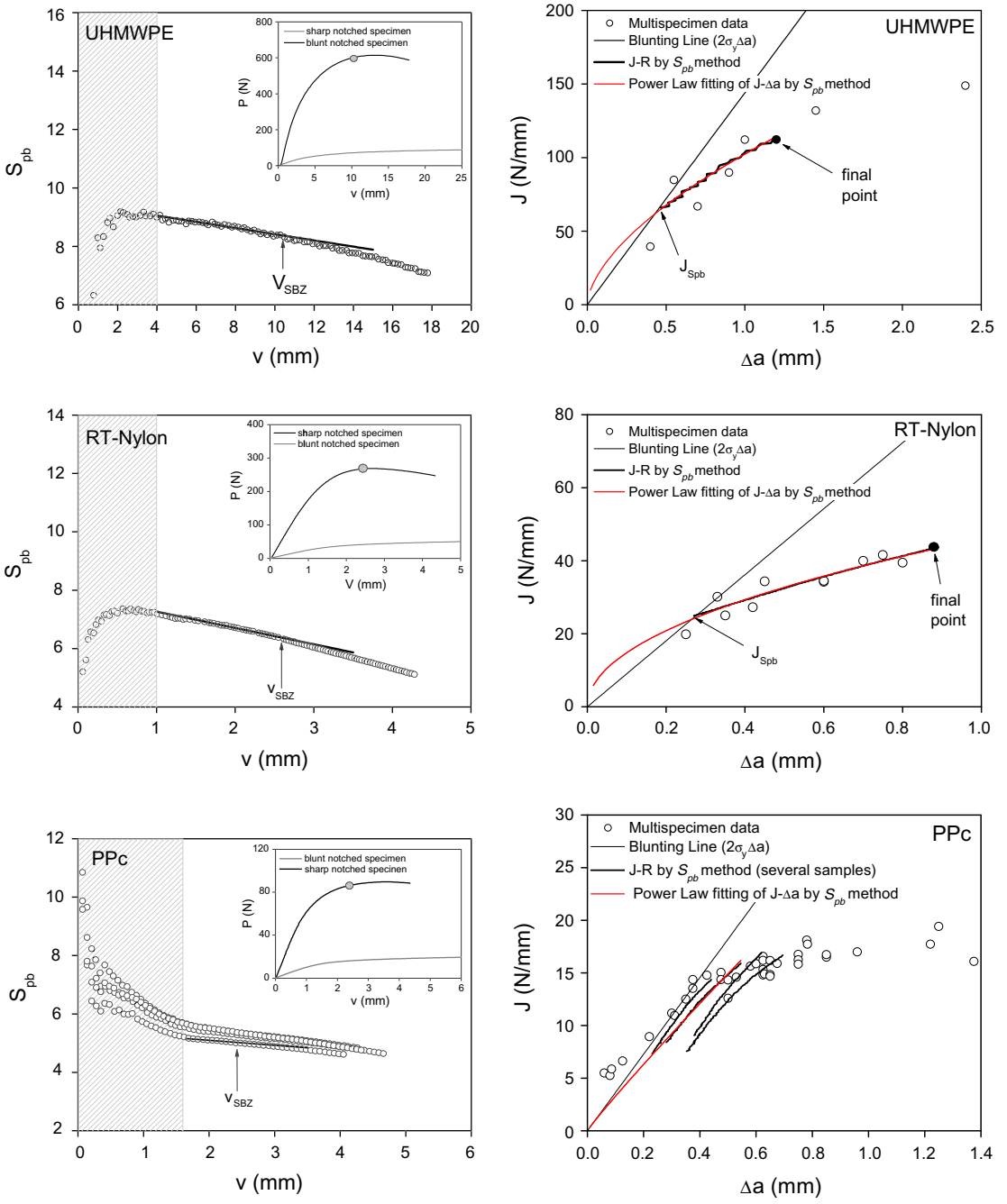

Fig. 5 (*continued*)

comparison of a blunt and a sharp notched samples. This limitation to methodology has been recently denounced in steel testing, as well [92]. An encouraging modification to S_{pb} method was proposed which aims to eliminate the spurious effect of the reference sample. This novel proposal has not been applied to polymers yet, but it may be considered a research challenge.

4.4. Normalization method J–R curves

Data reduction was executed according to Section 3.4. The measured force and displacement data were transformed into normalized force P_{Ni} and normalized displacement v_i, using the blunting crack length and the measured final crack length

Table 4
Summary of fracture toughness, and relevant values and parameters arisen from S_{pb} and Normalization methods.

Material	S_{pb} method				Normalization method	
	v_{SBZ} (mm)	m	$a_{f,p}$ // $a_{f,m}$ (mm) (relative error)	J_{Spb} (N/mm)	$J_{0.2,N}$ (N/mm)	Δa_f (mm) predicted (measured)
ABS	1.22	2.05	8.84 // 8.96 (1.3%)	5.3	7.0	0.74 (0.75)
HIPS	1.03	2.13	10.48 // 10.52 (0.4%)	3.0	3.9	0.62 (0.62)
RT-PMMA	0.91	1.89	9.39// 9.68 (3.0%)	4.5	2.7	0.80 (0.80)
UHMWPE	11.3	2.21	15.28 // 15.30 (0.1%)	65.9	37.9	1.14 (1.20)
RT-Nylon	2.7	1.90	7.29 // 7.28 (0.1%)	24.8	18.6	0.76 (0.80)
PPc[a]	2.56	2.18	6.94 // 7.00 (0.86%)	8.24	8.0	0.73 (0.75)

[a] Data arisen from one of the predicted curves are reported. See text for further analysis.

(see the included P_N–v plots in Fig. 7 – *left column*. All useful data were fitted to the Four parameter analytical function and the J–R curve was constructed. The deformation relationships developed in each case and the used range of displacement are shown in Fig. 7 – *left column*. Normalization J–R curves and multiple-specimen data are presented together in Fig. 7 – *right column*. In every case, the reproducibility was verified by fitting two separate specimens having essentially different crack extensions. Reliable J–R curves were obtained with the Normalization procedure for all of the materials studied but for PPc. Some oscillations at the beginning of the predicted J–R curves could eventually appear, being a typical issue of this methodology [93]. These oscillations can be overcome just replacing the initial part of the curve directly with the blunting line (Fig. 7 – *right column*). The use of the arbitrary 1% of plastic displacement to width ratio as the lower bound of the fitting range works well and it avoids the need of constructing an extra S_{pb} plot to define the so-called useful data range as previously proposed [46,94].

Obviously, a flat J–R curve cannot be predicted using the Normalization methodology. In particular for PPc the results of using different samples are shown in the Fig. 7 (PPc plot). Each experiment led to a different J–R curve. The reason of the failure of Normalization method may be simply found in the definition of the Material Key Curve. It relates univocally load, displacement and crack length. In a flat R curve a low degree of correlation between J values and crack growth exists. Let's say, that rising R curves are implicit in the Normalization method.

Regarding the suitability of Material Deformation Functions, additionally J–R curves for ABS and R-T nylon were developed using the power law function (Fig. 8a). The latter was widely used in the early beginning of application of Normalization methodology [48,50,67,95]. No general conclusions can be drawn from these scarce results. However, according to metals experience and the results already shown it can be said that the Four parameter analytical function can accurately capture the behavior of most of ductile materials and seems to be more versatile than power law and LMN functions for polymers [49].

Regarding the influence of the blunting line assumption (adopted k value) in the Normalization method prediction capability, we found that its influence is practically negligible (Fig. 8b), allowing the use of the theoretical value of 2 for predictive proposes. This result is in agreement with pervious findings [56,62,67] and in light contradiction with R. Varadarajan et al., who supported the use of power law function due to reduced sensitivity to the blunting assumption [55].

5. Conclusions

The following considerations emerge from the analysis of previous findings available in literature and results presented here.

The validity of Load Separation Principle in the load-plastic displacement range was previously demonstrated for a wide range of ductile polymers (see Table 1). Experiments shown in this paper broadens Load Separation validity to the whole range of displacement. This property allows the use of single specimen methods to *J-Integral* determination in polymers which, make use of a parameter ($\eta, \eta_{el}, \eta_{pl}$) capable of directly relate fracture energy with J. Besides, Load Separation provides an alternative method to calibrate η parameter of new geometries and/or to detect any material dependency of η formulas. In general, negligible material dependency was reported for fracture characterization of ductile polymers via *J-Integral* (see Table 1 and Fig. 2).

As a global conclusion it can be stated that Load Separation method and Normalization Data Reduction can be use to predict J–R curves from a single load versus displacement record (see Figs. 5 and 7, Tables 1 and 2). Both methods offer some advantages over the rigorous multiple-specimen technique. However, some problems and limitations in their application have been detected. Some of them are related with problems arising from the general application of J-criterion to polymers while others are inherent to the new methods themselves. Measuring final crack growth and describing the actual crack blunting behavior is still a question of debate in polymers.

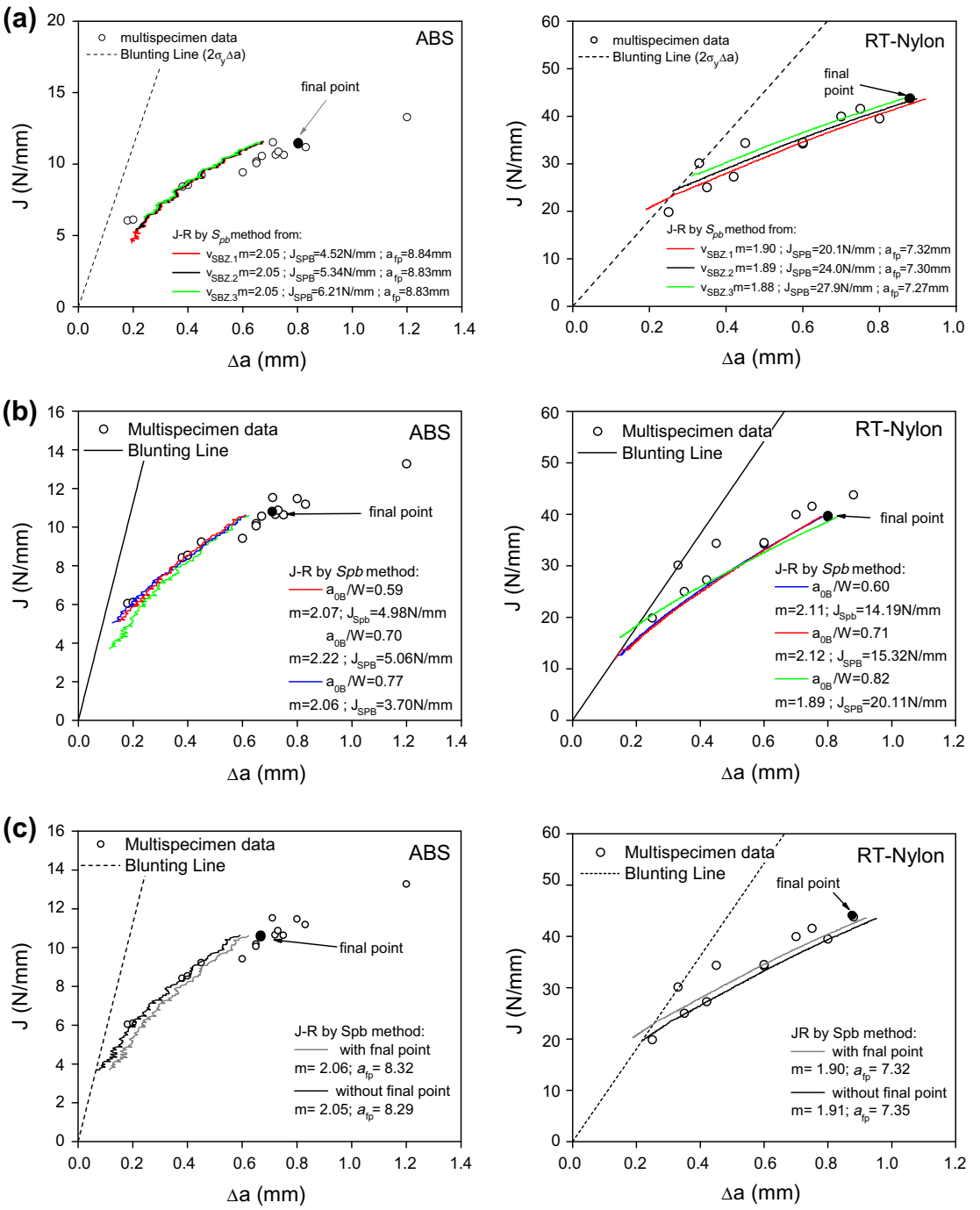

Fig. 6. S_{pb} method results for ABS (left column) and RT-Nylon (right column). Effect on the predicted *J–R* curves of: (a) accuracy on v_{SBZ} determination, (b) blunt notched depth and (c) final point exclusion for *m* parameter determination.

Normalization method yielded to *J–R* curves which practically superimposed the data obtained by the traditional multiple-specimen technique. It is known, that the quality of Normalization prediction is closely related with the pertinence of the selected deformation function, *H*. Our results confirm the versatility of the Four parameter analytical function proposed by ASTM test method E1820-01 in describing the stress strain behavior of materials with essentially different deformation patterns. Nonetheless, good agreement is found when using other functional forms, especially for the power law (see Table 2 and Fig. 8a). Four parameter analytical function and power law have an additional advantage over the traditional LMN function: they only use points on the Blunting line and the final point to fit the *H* function.

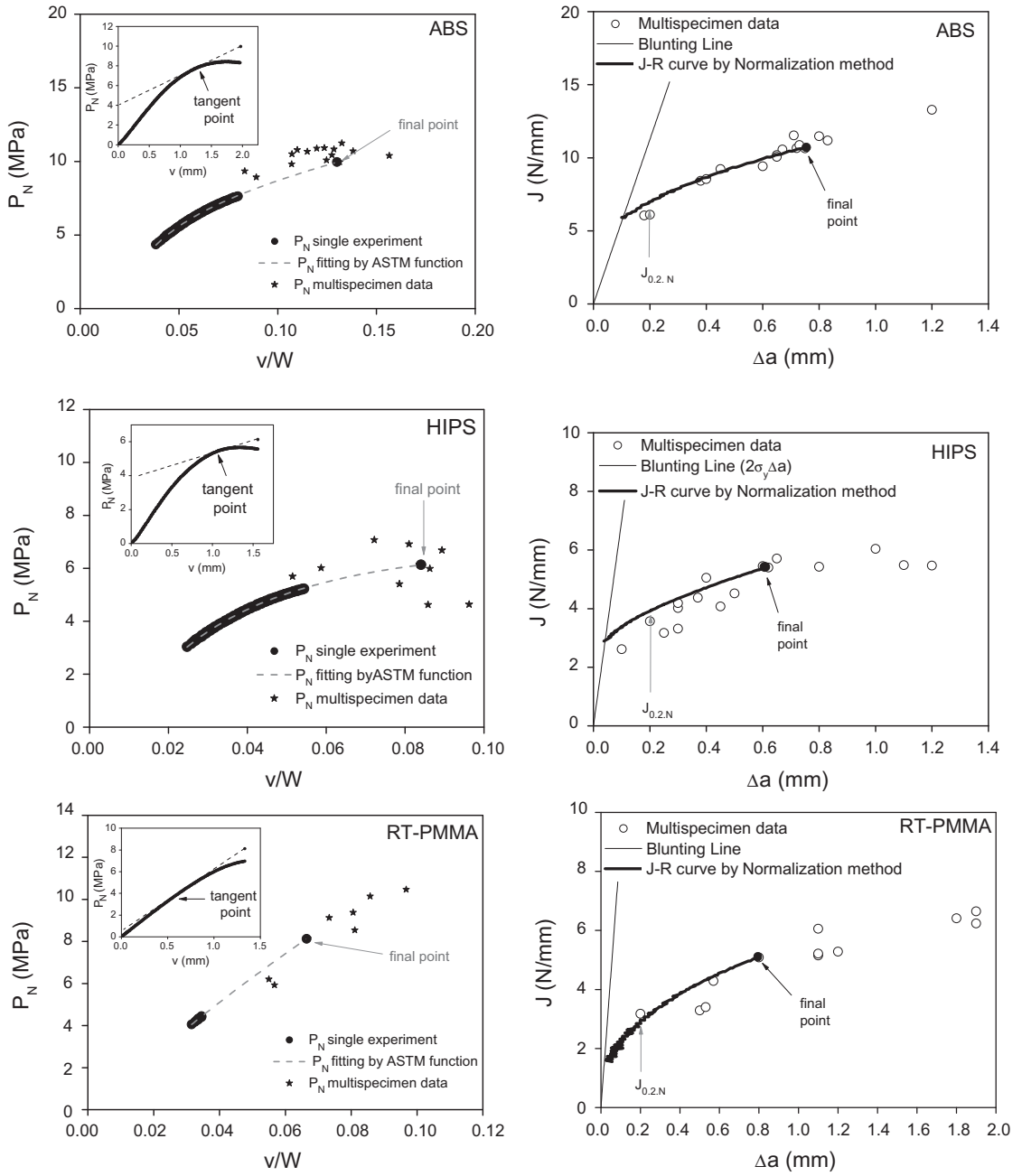

Fig. 7. Normalization method results: P_N vs. displacement plots (left column) and the corresponding constructed *J–R* curves (right column). P_N values from multi-specimen data were added but not included in the key curve fitting.

The version based on total displacement resulted very easy to apply since it obviates to convert raw load–displacement to load-plastic displacement data thus, eliminating iterative calculations.

Caution must be taken with materials having unknown blunting behavior since the quality of predictions may be dependent on the capability of the blunting behavior in describing crack growth before ductile tearing (see UHMWPE behavior in this paper). Anyway, apart from UHMWPE a good prediction was obtained by approximating behavior with ideal blunting behavior in many examples. It seems that the quality of Normalization prediction relies more on the accuracy of crack growth determination rather than on the blunting assumption.

Either the use of S_{pb} or the arbitrary 1% of plastic displacement to with ratio (Eq. (28)) to identify the onset of the separable region led to good results. This indicates that *J–R* curve is not sensitive to the extent of the region used for its construction provided this zone is included within the true separable blunting region.

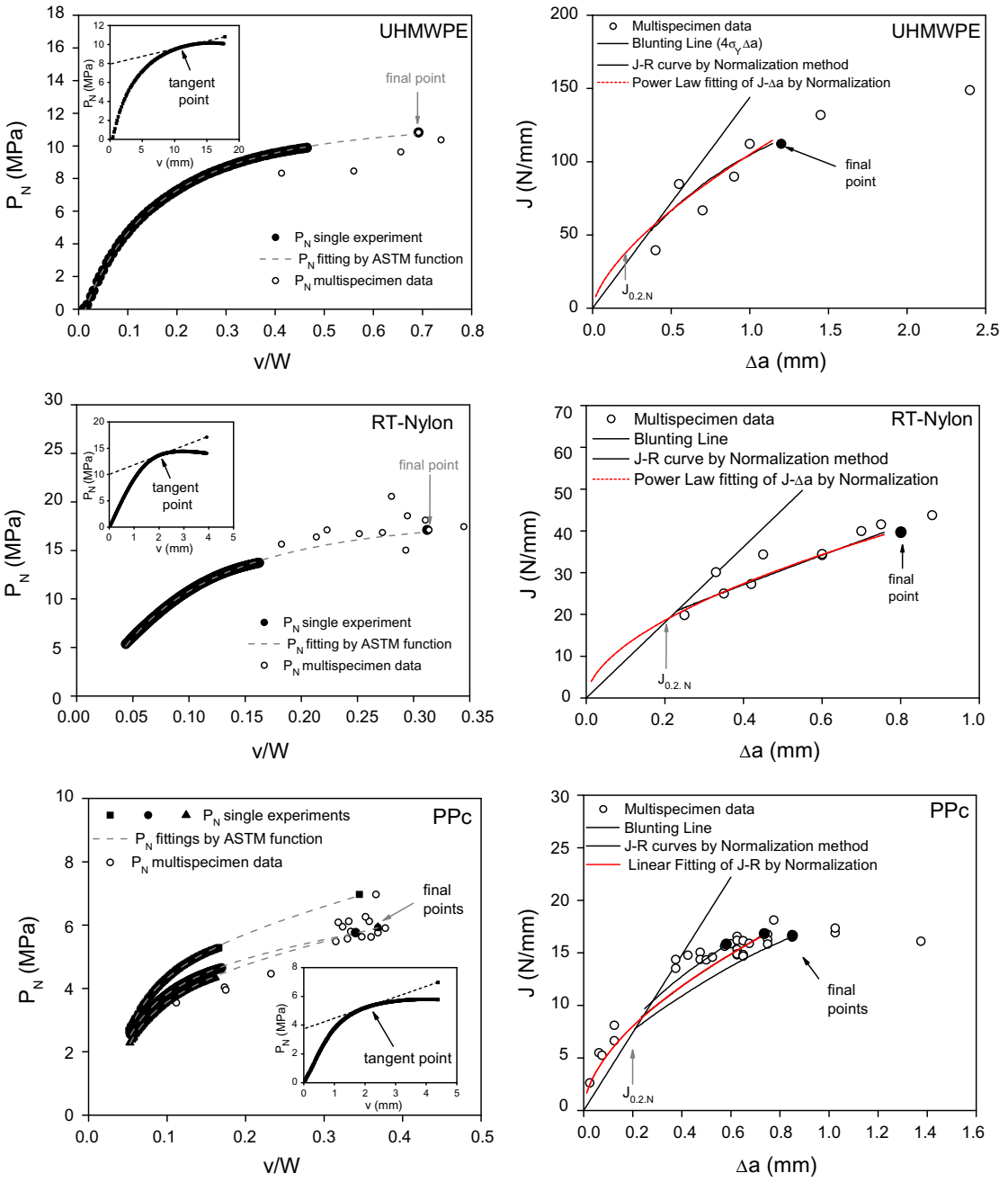

Fig. 7 (*continued*)

The appeal of the S_{pb} method is basically its strong theoretical background and its experimental simplicity. An acceptable agreement was found with *J–R* curves determined by the multiple-specimen technique in most of the cases analyzed being applicable to many polymers (see Table 1). In contrast with Normalization Data Reduction technique in which, the method accuracy relies heavily on accurate measurement of the load, displacement and crack length at the end of test [96], Load Separation method, still thrown consistent results when final point is not available [40,60,62,97]. So, Load Separation method could be helpful for cases where high loading rates are applied or where high temperatures or aggressive environments are used in which the final point is not always available.

Since Load Separation method bases its calculation on the comparison of two identical samples differing only in crack length and crack tip constraint, special care should be put in the preparation of the samples. Small errors in geometry could lead to sensible errors in *J–R* curve prediction. Conversely, the quality of inferred *J–R* curves was insensitive to the accuracy of the estimated *SBZ* range.

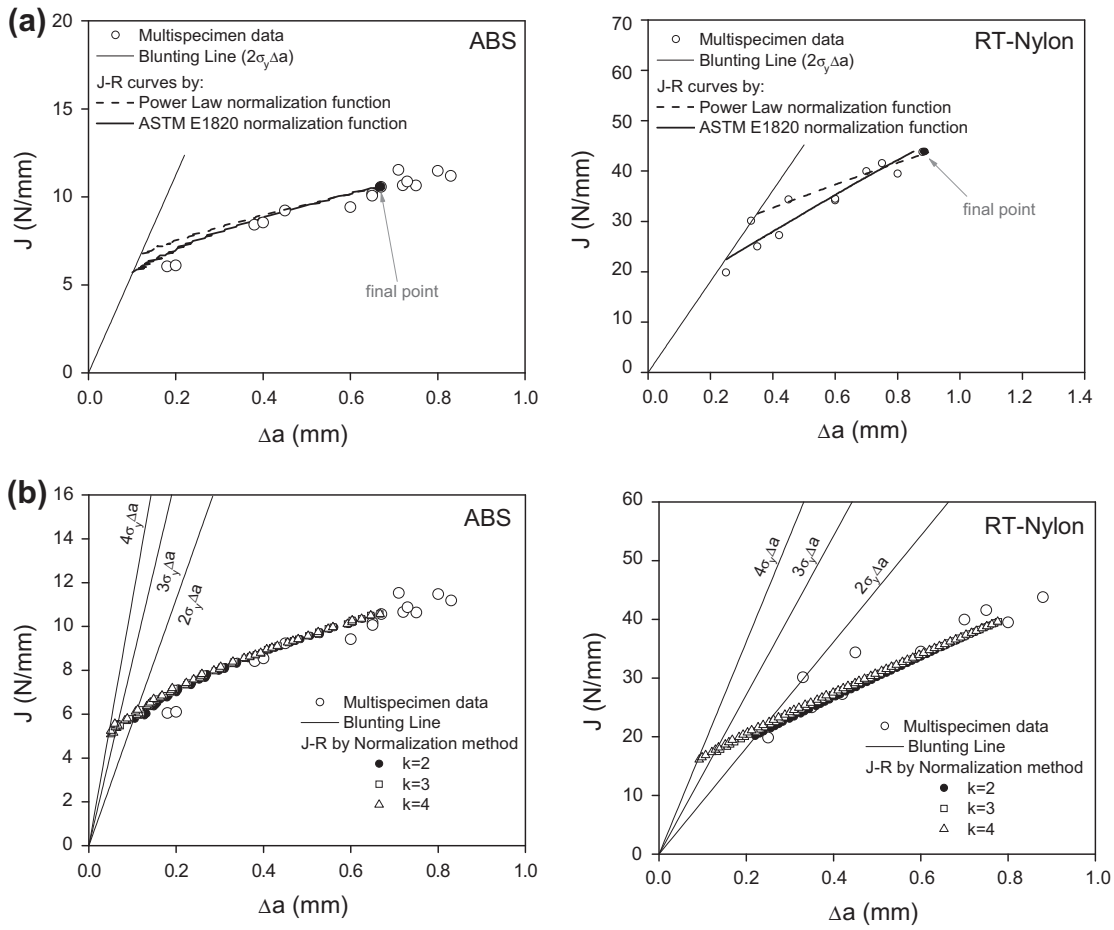

Fig. 8. Normalization method results for ABS (left column) and RT-Nylon (right column). Effect on the predicted *J–R* curves of: (a) key curve functional form assumption and (b) blunting behavior assumption.

Disappointedly, a reliable initiation fracture toughness parameter, J_{Spb}, taken as the value of J at the initiation of ductile tearing could not be determined following Sharobeam and Landes scheme [30] since J_{Spb} values depended on the blunt notch depth [92] of the reference sample.

Unfortunately, both Normalization and S_{pb} methods failed to predict *J–R-curves* of materials displaying flat *R*-curves, i.e. in which poor or none correlation exists between individual *J* values and crack growth length (see PPc in this paper). That is to say that rising *R*-curves are implicit in this kind of methodologies imposing a great limitation to single specimen techniques since actual behavior may not be known *a priori.*

There are few examples in literature in which Normalization or S_{pb} were directly adopted to qualify *J–R* behavior of novel materials [60,62,72,91]. Most of the papers are concerned with the development of these novel methodologies themselves rather than their direct application for materials characterization. This suggests that a "blind" round-robin putting together data from different laboratories appears mandatory in order to adopt both methodologies with more reliance as fracture characterization approaches.

A good example of the potential usefulness of both methods can be found in the development of novel polymeric products with tailored toughness when only small amounts of materials are available or to assay behaviors against processing conditions or under aggressive environments.

References

[1] Barany T, Czigany T, Karger-Kocsis J. Application of the essential work of fracture (EWF) concept for polymers, related blends and composites: a review. Prog Polym Sci 2010;35:1257–87.
[2] ASTM E1290-08E1: standard test method for crack-tip opening displacement (CTOD) fracture toughness measurement.
[3] Patel Y, Blackman BRK, Williams JG. Determining fracture toughness from cutting tests on polymers. Engng Fract Mech 2009;76:2711–30.
[4] Vipulanandan C, Dharmarajan N. Critical crack tip opening displacement for polymer composites. Engng Fract Mech 1989;33:409–19.

[5] Hale GE, Ramsteiner F. A testing protocol for conducting J-crack growth resistance curve tests on plastics. In: Moore CR, Pavan A, Williams JG, editors. Fracture mechanics testing methods for polymers, adhesives and composites, ESIS Publication 28, Oxford (UK): Elsevier Science Ltd.; 2001. p. 138–57.
[6] ASTM D6068-10: standard test method for determining J–R curves of plastic materials.
[7] ASTM E1820-09E1: standard test method for measurement of fracture toughness.
[8] Mai YW, Wong SC, Chen XH. Application of fracture mechanics for characterization of toughness of polymer blends. In: Paul DR, Bucknall CB, editors. Polymer blends. Performance, vol. 2. New York: Wiley-Interscience; 2000. p. 17–58.
[9] Williams JG. Fracture mechanics. In: Haward RN, Young RJ, editors. The physics of glassy polymers. London (UK): Chapman & Hall; 1997. p. 343–62.
[10] El-Badawy AA, Younan M. Elastic–plastic fracture mechanics for two-dimensional stable crack growth and instability as applied to PVC pipe material. In: Proceedings of the CSME mechanics in design; 1996. p. 913–22.
[11] Bernal CR, Lopez Montenegro H, Frontini PM. Failure prediction analysis for polyethylene flawed pipes. Engng Fract Mech 2003;70:2149–62.
[12] Begley JA, Landes JD. The J integral as a fracture criterion. In: Fracture toughness ASTM STP 514. Philadelphia: American Society for Testing and Materials; 1972. p. 1–23.
[13] Begley JA, Landes JD. The effect of specimen geometry on JIc. In: Fracture toughness. ASTM STP 514. Philadelphia: American Society for Testing and Materials; 1972. p. 24–39.
[14] Rice JR, Paris PC, Merkle, JG. Some further results on the J integral analysis. In: Progress in flaw growth and fracture toughness testing ASTM STP 536. Philadelphia: American Society for Testing and Materials; 1973. p. 231–45.
[15] Merkle JG, Corten HT. A J integral analysis for the compact specimen, considering axial force as well as bending effects. J Press Vessel Technol ASME Trans 1974:286–92.
[16] Sumpter JD, Turner CE. Methods for laboratory determination of J_c. In: Cracks and fracture ASTM STP 601. Philadelphia: American Society for Testing and Materials; 1976. p. 3–18.
[17] ASTM E813-89E01: Test method for J_{IC}. A measure of fracture toughness.
[18] Narisawa I. Fracture and toughness of crystalline polymer solids. Polym Engng Sci 1987;27:41–5.
[19] Huang DD, Williams JG. J testing of toughened nylons. J Mater Sci 1987;22:2503–8.
[20] Huang DD. The application of the multispecimen J-integral technique to toughened polymers. In: Elastic–plastic fracture test methods: the user's experience ASTM STP 1114. Philadelphia: American Society for Testing and Materials; 1991. p. 290–306.
[21] Bernal C, Frontini PM, Herrera R. Fracture toughness determination of ABS polymers using the J-method. Polym Test 1992;11:271–88.
[22] Martinatti F, Ricco T. High-rate J-testing of toughened polypropylene. Polym Test 1994;13:405–18.
[23] Tjong SC, Ke YC. Fracture toughening behavior of elastomer modified polyphenylene ether/polyamide blends. Eur Polym J 1998;34:1565–70.
[24] Seidler S, Grellmann W. Possibilities and limits of standards and drafts for J–R curve determination of polymers. In: Seidler S, Grellmann W, editors. Deformation and fracture behaviour of polymers. Berlin: Springer-Verlag; 2001. p. 87–94.
[25] Chiou KC, Chang FC, Mai YW. Fracture toughness characterizations of compatibilized polyamide-6 (PA6)/poly(phenylene ether) (PPE) blends. J Polym Res 2001;8:17–26.
[26] Graice IM, Younan MYA, Naga SAR. Experimental investigation into the fracture toughness of polyethylene pipe material. J Press Vessel Technol 2005;127:70–6.
[27] Arkhireyeva A, Hashemi S. Fracture behaviour of polyethylene naphthalate (PEN). Polymer 2002;43:289–300.
[28] Voss B, Mayville RA. The use of the partial unloading compliance method for the determination of J_i–R curves and J_{Ic}. In: Loss FJ, Wessel ET, editors. Elastic–plastic fracture test methods: the user's experience. ASTM STP 856. Philadelphia: American Society for Testing and Materials; 1985. p. 117–30.
[29] Chung WN, Williams JG. Determination of J_{Ic} for polymers using the single specimen method. In: Joyce JA, editor. Elastic–plastic fracture test methods: the user's experience. ASTM STP 1114, vol. 2. Philadelphia: American Society for Testing and Materials; 1991. p. 320–39.
[30] Sharobeam MH, Landes JD. The load separation and η_{pl} development in precracked specimen test records. Int J Fract 1993;59:213–26.
[31] Ernst HA, Paris PC, Landes JD. Estimations on J-integral and tearing modulus T from a single specimen test record. In: Fracture mechanics: thirteenth conference. ASTM STP 743. Philadelphia: American Society for Testing and Materials; 1981. p. 476–502.
[32] Sharobeam MH, Landes JD. The load separation criterion and methodology in ductile fracture mechanics. Int J Fract 1991;47:81–104.
[33] Joyce JA, Ernst H, Paris PC. Direct J–R curve analysis: a guide to the methodology. In: Fracture mechanics: twelfth National Symposium, ASTM STP 700. Philadelphia: American Society for Testing and Materials; 1980. p. 222–36.
[34] Ernst H, Paris PC, Rossow M, Hutchinson JW. Analysis of load–displacement relationships to determine J–R curve and tearing instability material properties. In: Smith CW, editor. Fracture mechanics ASTM STP 677. Blacksburg: American Society for Testing and Materials; 1979. p. 581–99.
[35] Herrera R, Landes JD. Direct J–R curve analysis of fracture toughness test. J Test Eval 1988;16:427–49.
[36] Herrera R, Landes JD. Direct J–R curve analysis: a guide to the methodology. In: fracture mechanics twenty-first symposium, ASTM STP 1074. Philadelphia: American Society for Testing and Materials; 1990. p. 24–43.
[37] Orange TW. Methods and models for R-curve instability calculations. In: Fracture mechanics twenty-first symposium, ASTM STP1074. Philadelphia: American Society for Testing and Materials; 1990. p. 545–59.
[38] Landes JD, Zhou Z, Lee K, Herrera R. Normalization method for developing J–R curves with the LMN function. J Test Eval 1991;19:305–11.
[39] Joyce JA. Analysis of a high rate round robin based on proposed annexes to ASTME 1820. J Test Eval 2001;29:329–51.
[40] Wainstein J, de Vedia LA, Cassanelli AN. A study to estimate crack length using the separability parameter S_{pb} in steels. Engng Fract Mech 2003;70:2489–96.
[41] Dzugan J, Viehrig HW. Application of the normalization method for the determination of J–R curves. Mater Sci Engng A 2004;387–389:307–11.
[42] Zhu XK, Joyce JA. J–resistance curve testing of HY80 steel using SE(B) specimens and normalization method. Engng Fract Mech 2007;74:2263–81.
[43] Kim YS, Matvienko YG, Jeong HC. Development of experimental procedure based on the load separation method to measure the fracture toughness of Zr–2.5Nb tubes. Key Engng Mat 2007;345–346:449–52.
[44] Graham SM. Validation of enhanced normalization as an improvement over the normalization and compliance ratio methods. Engng Fract Mech 2010;77:832–41.
[45] Kehi K. Investigation and modeling continuous woven of the elastic–plastic fracture behavior of fabrigreinforced ceramic composites. Int J Fract 2007;148:387–400.
[46] Bernal CR, Cassanelli AN, Frontini PM. A simple method for J–R curve determination in ABS polymers. Polym Test 1995;14:85–92.
[47] Bernal CR, Cassanelli AN, Frontini PM. The load separation criterion applied to ABS polymers. Polymer 1996;37:4033–9.
[48] Bernal CR, Montemartini PE, Frontini PM. The use of load separation criterion and normalization method in ductile fracture characterization of thermoplastics polymers. J Polym Sci Part B: Polym Phys 1996;34:1869–80.
[49] Che M, Grellmann W, Seidler S, Landes JD. Application of a normalization method for determining J–R curves in glassy polymer PVC at different crosshead speeds. Fatigue Fract Engng Mater Struct 1997;20(2):119–27.
[50] Bernal CR, Rink M, Frontini PM. Load separation principle in J–R curve determination of ductile polymers: a comparative analysis of the suitability of different materials deformation functions used in the normalization method. Macrom Symp 1999;147:235–48.
[51] García Brosa V, Bernal CR, Frontini PM. Calibration of fracture mechanics parameters and JR curve determination in polyethylene side-grooved arc-shaped specimens. Engng Fract Mech 1999;62:231–48.
[52] Joyce PJ, Joyce JA. Evaluation of the fracture toughness properties of polytetrafluoroethylene. Int J Fract 2004;127:361–85.
[53] Brown EN, Dattelbaum DM. Fracture and damage evolution in polymers. Nucl Weapons J 2006;2:1–7.
[54] Antich P, Vázquez A, Mondragon I, Bernal C. Mechanical behavior of high impact polystyrene reinforced with short sisal fibers. Composites Part A 2006;37:139–50.

[55] Varadarajan R, Dapp EK, Rimnac CM. Static fracture resistance of ultra high molecular weight polyethylene using the single specimen normalization method. Polym Test 2008;27:260–8.
[56] Rodríguez C, Maspoch ML, Belzunce FJ. Fracture characterization of ductile polymers through methods based on load separation. Polym Test 2009;28:204–8.
[57] Cassanelli AN, Ortiz H, Cocco R, de Vedia LA. A study for η plastic factor determination in AA 6061-T6 alloy. Engng Fract Mech 2001;68:501–11.
[58] Cassanelli AN, Ortiz H, Wainstein J, de Vedia LA. Separability property and load normalization in AA6061-T6 aluminum alloy. In: fatigue and fracture mechanics ASTM STP 1406. Philadelphia: American Society for Testing and Materials; 2002. p. 49–72.
[59] Wainstein J, Frontini PM, Cassanelli AN. J–R curve determination using the load separation parameter Spb method for ductile polymers. Polym Test 2004;23:591–8.
[60] Wainstein J, Fasce LA, Cassanelli A, Frontini PM. High rate toughness of ductile polymers. Engng Fract Mech 2007;74:2070–8.
[61] Salazar A, Rodríguez J, Segovia A, Martínez AB. Influence of the notch sharpening technique on the fracture toughness of bulk ethylene–propylene block copolymers. Polym Test 2010;29:49–59.
[62] Salazar A, Rodríguez J. The use of the load separation parameter Spb method to determine the J–R curves of polypropylenes. Polym Test 2008;27:977–84.
[63] Baldi F, Agnelli S, Riccò T. On the applicability of the load separation criterion in determining the fracture resistance (JIc) of ductile polymers at low and high loading rates. Int J Fract 2010;165:105–19.
[64] Wilson CD, Mani P. Plastic J-integral calculations using the load separation method for the center cracked tension specimen. Engng Fract Mech 2002;69:887–98.
[65] Matvienko YG. The load separation method in nonlinear fracture mechanics. In: Proceedings of 12th international conference on fracture, Ottawa, Canada; 2009 [CD-Room T31-007].
[66] ASTM E399-09E1. Standard test method for linear-elastic plane-strain fracture toughness K_{Ic} of metallic materials.
[67] Morhain C, Velasco JI. Determination of JR curve of polypropylene copolymers using the normalization method. J Mater Sci 2001;36:1487–99.
[68] Morhain C, Velasco JI. JR curve determination of magnesium hydroxide filled polypropylene using the normalization method. J Mater Sci 2002;37:1635–44.
[69] Landes JD, Zhou Z. Application of load separation and normalization methods for polycarbonate materials. Int J Fract 1993;63:383–93.
[70] Zhou Z, Landes JD, Huang DD. J–R curve calculation with the normalization method for toughened polymers. Polym Engng Sci 1994;34:128–234.
[71] Joyce JA. Fracture toughness evaluation of polytetrafluoroethylene. Polym Engng Sci 2003;43(10):1702–14.
[72] Joyce JA, Joyce PJ. Toughness characterization of a metal filled polytetrafluoroethylene using the J-integral. Engng Fract Mech 2004;71:2513–31.
[73] Sharobeam MH, Landes JD, Herrera R. Eta factors in elastic plastic fracture testing. In: User experience on fracture test methods. Orlando: American Society for Testing and Materials; 1989. p. 1.
[74] Pascaud RS, Evans WT, McCullagh PJJ, Fitzpatrick D. Critical assessment of methods for evaluating J_{IC} for medical grade ultra high molecular weight polyethylene. Polym Engng Sci 1997;37:11–7.
[75] ASTM D638-10. Standard test method for tensile properties of plastics.
[76] Brinson FH, Brinson LC. Polymer engineering science and viscoelasticity: an introduction. New York: Springer; 2008.
[77] Sharobeam MH, Landes JD, Herrera R. Development of eta factors in elastic-plastic fracture testing using a load separation technique. In: Elastic–plastic fracture test methods: the user's experience ASTM STP 1114. Philadelphia: American Society for Testing and Materials; 1991. p. 114–32.
[78] Landes JD, Begley JA. Test results from J-integral studies: an attempt to establish a J_{Ic} testing procedure. In: Fracture analysis ASTM STP 560. Philadelphia: American Society for Testing and Materials; 1974. p. 170–86.
[79] ASTM D6068-96. Standard test method for determining J–R curves of plastic materials.
[80] Lee CB, Lu ML, Chang FC. Fracture toughness of high-impact polystyrene based on three J-integral methods. J Appl Polym Sci 1993;47:1867–80.
[81] Theocaris PS, Kytopoulos V, Stassinakis C. Blunting of cracks of intermediate states of stress by scanning electron microscopy. J Mater Sci 1989;24:1121–7.
[82] Narisawa I, Takemori MT. Fracture toughness of impact-modified polymers based on the J-Integral. Polym Engng Sci 1989;29:671–8.
[83] Williams JG. Introduction to elastic–plastic fracture mechanics. In: Moore DR, Pavan A, Williams JG, editors. Fracture mechanics testing methods for polymers adhesives and composites. ESIS Publication, vol. 28. Oxford (UK): Elsevier Science; 2001. p. 119–22.
[84] Pettarin V, Churruca MJ, Felhös D, Karger-Kocsis J, Frontini PM. Changes in tribological performance of high molecular weight high density polyethylene induced by the addition of molybdenum disulphide particles. Wear 2010;269:31–45.
[85] Salazar A, Garrido MA, Rodríguez J, Martínez AB. Determination of the J–R curves of ethylene-propylene block copolymers by means of different J-integral methodologies. Anales de Mecánica de la Fractura 2010;27(2):673–8.
[86] Baldi F, Ricco T. High-rate J-testing of toughened polyamide 6/6: applicability of the load separation criterion and the normalization method. Engng Fract Mech 2005;72:2218–31.
[87] Joyce JA. J–resistance curve testing of short crack bend specimens using unloading compliance. In: Fracture mechanics: twenty-second symposium, vol. I. ASTM STP 1131. Philadelphia: American Society for Testing and Materials; 1992. p. 904–24.
[88] ASTM E 1820-01. Standard test method for measurement of fracture toughness. Annual book of ASTM standards, vol. 03.01. West Conshohocken (PA): American Society for Testing and Materials; 2005 [Annex 15].
[89] Donoso JR, Landes JD. Common format for developing calibration curves in elastic–plastic fracture mechanics. Engng Fract Mech 1994;47(5):619–28.
[90] Cassanelli AN, Cocco R, de Vedia LA. Separability property and η_{pl} factor in ASTM A387-Gr22 steel plate. Engng Fract Mech 2003;70:1131–42.
[91] Frontini PM, Rueda F, Fasce LA. J–R curves of rubber modified polystyrenes: the use of load separation parameter to determine instantaneous crack lengths. In: Proceedings of 12th international conference of fracture, Ottawa, Canada; 2009 [CD T37.005].
[92] Bao C, Cai LX. Estimation of the J–resistance curve for Cr_2Ni_2MoV steel using the modified load separation parameter Spb method. J Zhejiang Univ – Sc A (Appl Phys Engng) 2010;11(10):782–8.
[93] Scibetta M, Lucon E, Schuurmans J, van Walle E. Numerical simulations to support the normalization data reduction technique. Engng Fract Mech 2006;73:524–34.
[94] Cassanelli AN, de Vedia LA. A proposed method for the applicability of load separation condition in precracked specimens. Int J Fract 1997;83(2):167–73.
[95] Baldi F, Riccò T. Applicability of the load separation criterion and the Normalization method to high-rate J testing of ductile polymers. In: Proceedings of 11th international conference of fracture, Turin, Italy, 2005 [CD 3240].
[96] Graham SM, Stiles DJ. An enhanced normalization method for dynamic fracture toughness testing. Fract Nano Engng Mater Struct 2006;B.2T15:461–2.
[97] Wainstein J, Fasce LA, Cassanelli A, Frontini PM. Impact fracture toughness determination of ductile polymers by Spb method. In: Proceedings of 16th European conference of fracture, Alexandropolis, Greece, 2006.